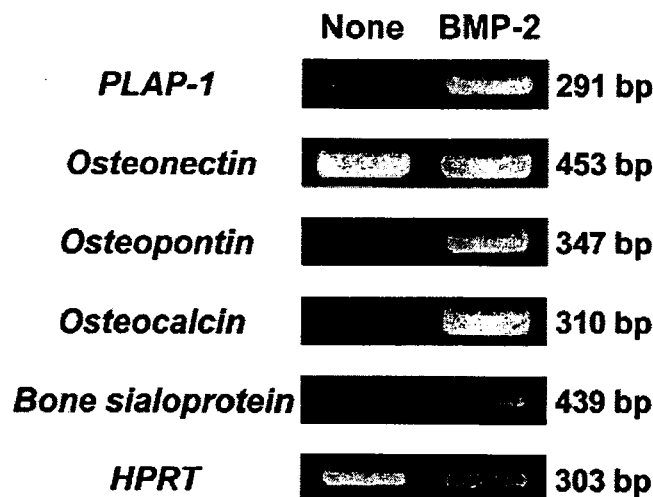


**Figure 2.** Effects of various cytokines on *PLAP-1* mRNA expression in PDL cells. After FCS deprivation for 48 hrs, human PDL cells were stimulated with indicated cytokines for another 48 hrs. Cells were harvested, and RNA was isolated for real-time RT-PCR analysis. Results are presented as the ratio of the amount of *PLAP-1* mRNA divided by *HPRT* mRNA. The values are given as means  $\pm$  standard deviations (SD) of quadruplicate assays. \* $P < 0.005$ ,  $n = 4$ , compared with None.

differentiated into hard-tissue-forming cells, and calcified nodule formation was finally observed in the culture (data not shown). We also confirmed that the addition of FGF-2 in the late stage of this long-term culture resulted in down-regulation of ALPase activity (Takayama *et al.*, 1997) (Fig. 1A) and inhibited the calcified nodule formation (data not shown). We performed real-time RT-PCR analysis of *PLAP-1* using RNAs isolated from the PDL cells harvested on day 0 and day 20, with or without FGF-2 stimulation (Fig. 1B). Expression of *PLAP-1* was increased during the culture in mineralization media, and strong expression was detected on day 20. The transcription of *PLAP-1* was clearly decreased in the PDL cells cultured in the presence of FGF-2 from day 15 (Fig. 1B), accompanying the down-regulation of their ALPase activity (Fig. 1A.). The transcription of *Biglycan* and *Decorin* also tended to be suppressed by stimulation with FGF-2. However, the expression of *Biglycan* mRNA and *Decorin* mRNA during the culture was changed only slightly, compared with that of *PLAP-1* mRNA (Fig. 1B).

### Up-regulation of *PLAP-1* mRNA Expression by BMP-2

We examined the effects of several other cytokines, assumed to be involved in the process of cytodifferentiation of PDL cells, on *PLAP-1* expression. Human PDL cells were stimulated with FGF-2, PDGF-BB, BMP-2, BMP-4, HGF, or EGF for 48 hrs, as described in MATERIALS & METHODS, and were examined for expression of *PLAP-1* mRNA by real-time RT-PCR analysis (Fig. 2). We used the optimum concentration for each cytokine, which induced proliferation of PDL cells equally (data not shown). The real-time RT-PCR analysis showed that FGF-2 and PDGF-BB significantly down-regulated the expression of *PLAP-1* mRNA in PDL cells. In contrast, BMP-2 and BMP-4, which strongly induced



**Figure 3.** mRNA induction of *PLAP-1* and mineralization-related genes in PDL cells by BMP-2. After FCS deprivation for 48 hrs, human PDL cells were stimulated with 100 ng/mL of BMP-2 for another 48 hrs. Cells were harvested, and RNA was isolated for RT-PCR analysis. The numbers of PCR cycles were: 24 for *PLAP-1*, 21 for *Osteonectin*, 37 for *Osteopontin*, 37 for *Osteocalcin*, 37 for *Bone sialoprotein*, and 27 for *HPRT*. The sizes of PCR products are shown on the right of each panel. Similar results were obtained in 3 separate experiments, and representative data are shown.

mineralization of PDL cells, significantly up-regulated *PLAP-1* transcription. In contrast, neither HGF nor EGF changed the expression of *PLAP-1* mRNA in PDL cells.

We then examined the regulation of the expression of *PLAP-1* mRNA by BMP-2 in detail. Human PDL cells were stimulated with various concentrations of BMP-2 for 48 hrs, and were examined by RT-PCR analysis for the expression of *PLAP-1*. Stimulation of PDL cells with BMP-2 resulted in increased expression of *PLAP-1* mRNA in a dose-dependent manner (data not shown).

We then confirmed the effects of BMP-2 on the induction of the mineralization and cytodifferentiation of PDL cells by investigating the gene expression of mineralization-related proteins (Fig. 3). PDL cells were stimulated with BMP-2 (100 ng/mL) for 48 hrs, and RNA was isolated from the cells. RT-PCR analysis revealed that the transcription of *PLAP-1* was induced along with *Osteopontin*, *Osteocalcin*, and *Bone sialoprotein* transcripts by the stimulation of BMP-2 (Fig. 3).

### Induction of *PLAP-1* Protein by BMP-2 in PDL Cells

*PLAP-1* protein had a sequence similar to that of *Decorin* and *Biglycan* (Yamada *et al.*, 2001). To generate a polyclonal antibody specific for *PLAP-1* protein, we carried out protein alignment of these 3 proteins to find amino acid sequences unique and antigenic for generating anti-*PLAP-1* antibodies (Fig. 4A). Fig. 4A shows the peptide sequences which we selected for the immunization of rabbits. We cultured human PDL cells for 48 hrs in the presence or absence of BMP-2, and stained the cells with the polyclonal antibody (Fig. 4B). During the whole staining process, the PDL cells were alive and not fixed. The cell surface of BMP-2-stimulated PDL cells was stained with the anti-*PLAP-1* polyclonal antibody in a dose-dependent manner (Fig. 4Ba-c). No staining was observed in the negative control, in which pre-immune rabbit serum was

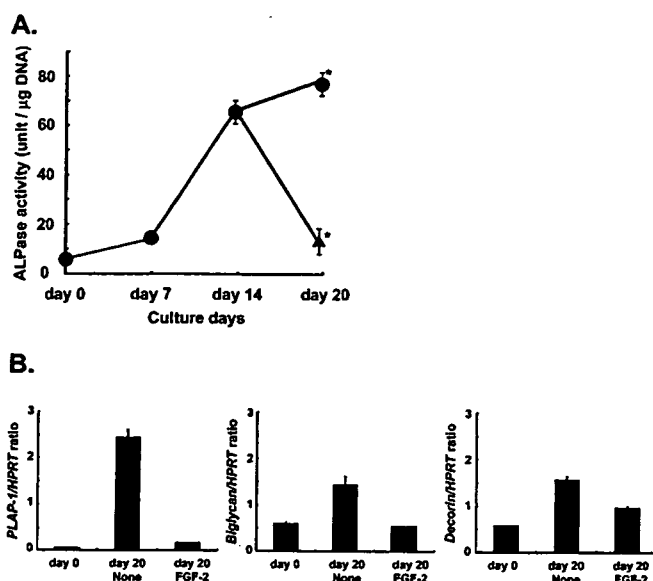


**Figure 1.** Real-time RT-PCR analysis of *PLAP-1* mRNA expression in the process of cytodifferentiation of human PDL cells. **(A)** ALPase activity of PDL cells. Human PDL cells were cultured in the presence of 10 mM  $\beta$ -glycerophosphate and 50  $\mu$ g/ml ascorbic acid. Triangle shows ALPase activity of PDL cells cultured in the presence of FGF-2 (20 ng/ml) from day 15 in the cultured period. Circles show ALPase activities of PDL cells cultured without FGF-2. The values are given as means  $\pm$  standard deviations (SD) of triplicate assays. \* $P < 0.05$ ,  $n = 3$  vs. respective PDL cells on day 20. **(B)** Down-regulation of *PLAP-1* mRNA of PDL cells by FGF-2. RNA from the same samples in panel A was reverse-transcribed into cDNA. Expression of specific mRNAs was detected by real-time PCR with primers specific for *PLAP-1*, *Biglycan*, *Decorin*, and *HPRT*. Results are presented as the ratio of the amount of each SLRP mRNA divided by *HPRT* mRNA. The values are given as means  $\pm$  standard deviations (SD) of triplicate assays.

MO, USA) (50 ng/mL), BMP-2 (Genzyme/Techne, Minneapolis, MN, USA) (100 ng/mL), BMP-4 (Genzyme/Techne) (100 ng/mL), hepatocyte growth factor (HGF) (SIGMA) (100 ng/mL), or epidermal growth factor (EGF) (SIGMA) (100 ng/mL) and incubated for another 48 hrs. The stimulated cells were then harvested, and total RNA was isolated for RT-PCR analysis.

### RT-PCR Analysis

Primers for real-time RT-PCR analysis were designed with Perfect Real Time Primer Design software (TAKARA, Shiga, Japan). Primers for *PLAP-1* were: (sense) 5'-GGGTGACGGTGTCCATATCAG-3' and (antisense) 5'-TGAAGCTCCAATAAAGTTGGTGGTA-3'. Primers for *Biglycan* were: (sense) 5'-CAACCAGATCAGGATGATCGAGAA-3' and (antisense) 5'-CCCATGGGACAGAAGTCGTTG-3'. Primers for *Decorin* were: (sense) 5'-GGGAGCTTCACTTGGACAACAAC-3' and (antisense) 5'-GGGCAGAAGTCACTTGATCCAAC-3'. Primers for *hypoxanthine-guanine phosphoribosyl transferase (HPRT)* were: (sense) 5'-CCAGACAAGTTTGTGTAGG-3' and (antisense) 5'-TCCAACTCAACTGAACTC-3'. Real-time RT-PCR reaction was carried out with a SYBR RT-PCR Kit (TAKARA) and performed with Smart Cycler version II (TAKARA). The amount of mRNA was calculated for each sample from the standard curve via the instrument software.

Semi-quantitative RT-PCR was performed according to the procedures described previously (Yamada et al., 2001). RT-PCR primers for *Osteonectin* were: (sense) 5'-GGAAGAACTGTGG

CAGAGGTGAC-3' and (antisense) 5'-TGTTGTCCTCATCCC TCTCATAACAG-3'. Primers for *Osteopontin* were (sense) 5'-CCAAGTAAGTCCAACGAAAG-3' and (antisense) 5'-GGTGATGTCCTCGTCTGTA-3'. Primers for *Osteocalcin* were: (sense) 5'-CATGAGAGCCCTCACA-3' and (antisense) 5'-AGAGCGACACCCTAGAC-3'. Primers for *Bone sialoprotein* were: (sense) 5'-GCCTGTGCTTCTCAATG-3' and (antisense) 5'-TTCCTTCCTTCTCCTCCTC-3'. Primers for *HPRT* were: (sense) 5'-CGAGATGTGATGAAGGAGATGGG-3' and (antisense) 5'-GCCTGACCAAGGAAAGCAAAGTC-3'.

### In vitro Assay for Alkaline Phosphatase (ALPase) Activity

Human PDL cells were cultured with the standard medium (see above) in the presence of 10 mM  $\beta$ -glycerophosphate and 50  $\mu$ g/mL ascorbic acid (mineralization medium). Cellular DNA content and ALPase activity in the PDL cells were determined according to the procedures described previously (Takayama et al., 1997).

### Production of Anti-PLAP-1 Antibody

A peptide (EPRSHFFPFD) homologous to human PLAP-1 was synthesized with a Model 430 A peptide synthesizer (Applied Biosystems). The peptide was conjugated to keyhole limpet hemocyanin (KLH) and used for the immunization of rabbits. This animal experiment was carried out in accordance with the guidelines for animal experimentation approved by the Japanese Association for Laboratory Animal Science.

### Immunocytochemical Staining

Human PDL cells grown to confluence in a 60-mm poly-L-lysine-coated glass-bottomed dish (Matsunami Glass, Osaka, Japan) were stimulated with BMP-2 for 48 hrs. Cells were washed with PBS 3 times and incubated with anti-PLAP-1 polyclonal antibody or pre-immune rabbit serum as a control at 4°C for 15 min. Cells were then incubated with biotinylated goat anti-rabbit IgG (H+L) antibody (Vector Laboratories, Burlingame, CA, USA) at 4°C for 15 min, and, finally, streptavidin-Alexa Fluor 488 (Molecular Probe, Engene, OR, USA) was added for the detection of immunoreactivity. Cells were washed 3 times with PBS after each step.

For the pre-incubation assay, we pre-incubated the anti-PLAP-1 polyclonal antibody with the antigenic KLH-conjugated PLAP-1 peptide, KLH alone, recombinant human Decorin (R&D Systems, Minneapolis, MN, USA), or recombinant human Biglycan (ABNOVA, Taipei, Taiwan) at room temperature for 15 min before staining BMP-2-stimulated PDL cells. In each pre-incubation assay, a 30-mg quantity of KLH-conjugated peptide or recombinant proteins was added to 1 mL of the anti-PLAP-1 antibody. The amount of peptide and recombinant proteins (30 mg/1 mL of anti-PLAP-1 antibody) was equivalent to the amount of total protein in the anti-PLAP-1 polyclonal antibody serum.

### Statistical Analysis

Data are expressed as means  $\pm$  standard deviations. The statistical significance of differences between 2 means was examined by the Mann-Whitney U test, and P values less than 0.05 were considered to indicate a significant difference.

## RESULTS

### Down-regulation of *PLAP-1* Gene Expression by FGF-2

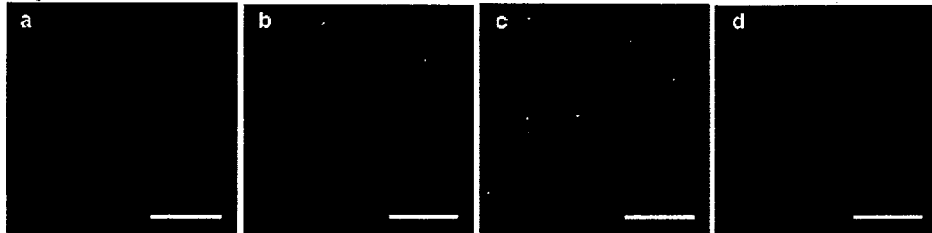
When human PDL cells were cultured in the mineralization media for 20 days, ALPase activity in the PDL cells was gradually increased (Fig. 1A). The PDL cells simultaneously

**A.**

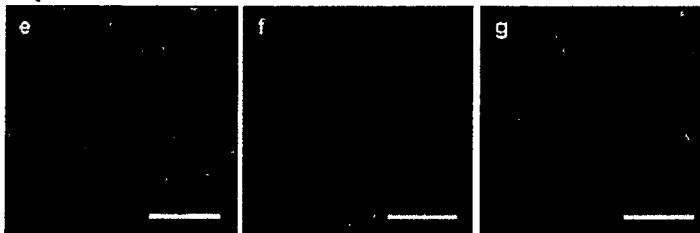
PLAP-1	60	PTRE	<b>SPFSSHIDPQDIL</b>	LFP	MCP	FGC	QCY	SRV	VHC	SDL	GLT	96		
Biglycan	57	PTYS	-----	AM	CP	FG	CH	CH	LR	VV	QC	SDL	GLK	82
Decorin	48	PSLG	-----	PV	CP	FR	CQ	CH	LR	VV	QC	SDL	GLD	73

**B.**

**Exp. I**



**Exp. II**



**Exp. III**

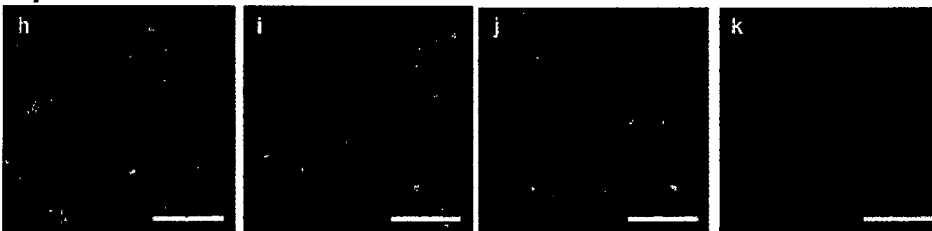


**Figure 4.** Induction of PLAP-1 protein on PDL cells by BMP-2. (A) Alignment of N-terminal of PLAP-1, Biglycan, and Decorin protein. The peptide sequence for antigen to immunize rabbits is shown in the dark-shaded box. (B) **Experiment I:** Immunocytochemical detection of PLAP-1 protein on PDL cells stimulated with BMP-2. Human PDL cells cultured in the glass-bottomed dish were stimulated with the different concentrations of BMP-2 for 48 hrs. The cells were washed with PBS and incubated with the anti-PLAP-1 polyclonal antibody or pre-immune rabbit serum, followed by the biotinylated goat anti-rabbit IgG mAb and then with streptavidin-Alexa Fluor 488. (a) No BMP-2 stimulation. (b) BMP-2 stimulation (200 ng/mL). (c) BMP-2 stimulation (400 ng/mL). (d) BMP-2 stimulation (400 ng/mL), staining with pre-immune rabbit serum. **Experiment II:** Dose-dependent inhibition of PLAP-1 staining with the PLAP-1 antigenic peptide. The anti-PLAP-1 polyclonal antibody was pre-incubated with different concentrations of the PLAP-1 peptide before BMP-2-stimulated (in 400 ng/mL) PDL cells were stained. (e) No PLAP-1 peptide. (f) Pre-incubation with the PLAP-1 peptide (30 mg/1 mL of anti-PLAP-1 antibody). (g) Pre-incubation with the PLAP-1 peptide (15 mg/1 mL of anti-PLAP-1 antibody). **Experiment III:** No cross-reaction of the anti-PLAP-1 antibody to Decorin or to Biglycan. The anti-PLAP-1 antibody was pre-incubated with either recombinant Decorin or Biglycan before BMP-2-stimulated (in 400 ng/mL) PDL cells were stained. (h) No pre-incubation. (i) Pre-incubation with recombinant Decorin (30 mg/1 mL of anti-PLAP-1 antibody). (j) Pre-incubation with recombinant Biglycan (30 mg/1 mL of anti-PLAP-1 antibody). (k) Pre-immune rabbit serum staining. Representative data of 3 independent experiments are shown. Scale bars = 50  $\mu$ m.

used as the primary antibody (Fig. 4Bd). We then pre-incubated the antibody before staining the BMP-2-stimulated PDL cells with different amounts of the PLAP-1 antigenic peptide, which we utilized for immunization. Pre-incubation of the PLAP-1 antigenic peptide inhibited the binding of the antibody to BMP-2-stimulated PDL cells in a dose-dependent manner (Fig. 4Be~g). No inhibition was observed in the negative control in which only KLH carrier protein was used for the pre-incubation

with the antibody (data not shown). Moreover, we pre-incubated the anti-PLAP-1 antibody with either recombinant human Decorin or recombinant human Biglycan before staining the BMP-2-stimulated PDL cells (Fig. 4Bh~k). No inhibition was observed by the pre-incubation with either recombinant Decorin or recombinant Biglycan.

## DISCUSSION

In this study, we analyzed the regulation of PLAP-1 expression in human PDL cells by mineralization-related cytokines. The transcription of *PLAP-1* was up-regulated along with the cytodifferentiation process of PDL cells and down-regulated when the process was arrested by FGF-2 (Fig. 1). This suggests that *PLAP-1* expression is closely associated with the process of cytodifferentiation of PDL cells. FGF-2 and PDGF-BB, which have mitogenic and chemotactic activities (Rifkin and Moscatelli, 1989; Hoch and Soriano, 2003), clearly suppressed the expression of *PLAP-1* in PDL cells (Fig. 2). Since PDL cells proliferate after stimulation with FGF-2 or PDGF-BB, *PLAP-1* may not be essential for cell proliferation. In contrast, BMP-2 and BMP-4 clearly induced the expression of *PLAP-1* (Fig. 2). BMP-2 is one of the most potent cytokines that stimulate osteoblast differentiation and bone formation (Hogan, 1996; Canalis *et al.*, 2003). BMP-2 has also been reported to stimulate osteoblastic differentiation in human PDL cells (Kobayashi *et al.*, 1999), and to promote dental follicle cells, putative progenitor cells for the periodontium, to induce differentiation into a cementoblastic/osteoblastic phenotype (Zhao *et al.*, 2002). Given that BMP-2 induced the cytodifferentiation and mineralization of PDL cells, PLAP-1 is closely associated with the cytodifferentiation of PDL cells into hard-tissue-forming cells. BMP-2 induced the expression of *PLAP-1* in a dose-dependent manner. *PLAP-1* was then transcribed along with the induction of other BMP-2-induced mineralization-related genes (Fig. 3). These results suggest that PLAP-1 is a mineralization-related gene, and that its transcription might be driven by the BMP-2 signaling pathway.

Recently, it was demonstrated that topical application of recombinant FGF-2 or PDGF-BB enhances the healing process and accelerates periodontal tissue regeneration (Takayama *et al.*, 2001; Murakami *et al.*, 2003; Nevins *et al.*, 2003). In the *in vivo* process of periodontal tissue regeneration, FGF-2 is likely to generate a suitable micro-environment in the FGF-2-applied sites by regulating the production of extracellular matrix (Takayama *et al.*, 1997; Shimabukuro *et al.*, 2005). Interestingly, we found that both FGF-2 and PDGF-BB strongly suppressed transcription of *PLAP-1* in PDL cells (Fig. 2). Thus, the effects of FGF-2 and PDGF-BB on periodontal tissue regeneration might be partly associated with suppression of *PLAP-1* expression in PDL. Temporal reduction of *PLAP-1* during the early phase of wound healing might be suitable for periodontal tissue regeneration in terms of the creation of an ideal micro-environment at the site.

*PLAP-1* is categorized into the same subclass of SLRP proteoglycan families as Biglycan and Decorin (Yamada *et al.*, 2001). Biglycan and Decorin were dominantly expressed in bone and connective tissue of skin, respectively (Ameys and Young, 2002). In general, both proteoglycans exist ubiquitously in mineralized tissues and connective tissues. In oral tissues, Biglycan is expressed in odontoblasts and ameloblasts and regulates the cytodifferentiation of those cells (Iozzo, 1997). Decorin is expressed ubiquitously in tissues of the periodontium (Hakkinen *et al.*, 1993). However, we could not detect the *PLAP-1* transcript in bone tissue by Northern blot analysis, but its expression was specifically revealed in PDL by *in situ* hybridization (Yamada *et al.*, unpublished observations). Changes in *Decorin* and *Biglycan* were slight in the course of cytodifferentiation of PDL cells, compared with *PLAP-1* expression (Fig. 1). These findings suggest that *PLAP-1* has unique function(s) in the PDL, compared with those of *Decorin* and *Biglycan*, and may play different roles in the process of the cytodifferentiation of the PDL cells.

The present findings demonstrated that the *PLAP-1* transcript is tightly regulated by FGF-2 and BMP-2 and closely associated with the process of cytodifferentiation and mineralization of human PDL cells. Thus, *PLAP-1* is expected to be useful for our understanding of the molecular basis of periodontal ligament functions.

## ACKNOWLEDGMENTS

This work was supported by Grants-in-Aid from the Japan Society for the Promotion of Science (15590646, 17209065, 17390560, and 17390561) and was part of the 21st Century COE entitled "Origination of Frontier BioDentistry" at the Osaka University Graduate School of Dentistry, supported by the Ministry of Education, Culture, Sports, Science and Technology.

## REFERENCES

- Ameys L, Young MF (2002). Mice deficient in small leucine-rich proteoglycans: novel *in vivo* models for osteoporosis, osteoarthritis, Ehlers-Danlos syndrome, muscular dystrophy and corneal disease. *Glycobiology* 12:107R-116R.
- Canalis E, Economides AN, Gazzerro E (2003). Bone morphogenetic proteins, their antagonists, and the skeleton. *Endocr Rev* 24:218-235.
- Hakkinen L, Oksala O, Salo T, Rahemtulla F, Larjava H (1993). Immunohistochemical localization of proteoglycans in human periodontium. *J Histochem Cytochem* 41:1689-1699.
- Henry SP, Takanosu M, Boyd TC, Mayne PM, Eberspaecher H, Zhou W, *et al.* (2001). Expression pattern and gene characterization of asporin, a newly discovered member of the leucine-rich repeat protein family. *J Biol Chem* 276:12212-12221.
- Hoch RV, Soriano P (2003). Roles of PDGF in animal development. *Development* 130:4769-4784.
- Hogan BL (1996). Bone morphogenetic proteins: multifunctional regulators of vertebrate development. *Genes Dev* 10:1580-1594.
- Iozzo RV (1997). The family of the small leucine-rich proteoglycans: key regulators of matrix assembly and cellular growth. *Crit Rev Biochem Mol Biol* 32:141-174.
- Kobayashi M, Takiguchi T, Suzuki R, Yamaguchi A, Deguchi K, Shionome M, *et al.* (1999). Recombinant human bone morphogenetic protein-2 stimulates osteoblastic differentiation in cells isolated from human periodontal ligament. *J Dent Res* 78:1624-1633.
- Lorenzo P, Aspberg A, Onnerfjord P, Bayliss MT, Neame PJ, Heinegard D (2001). Identification and characterization of asporin, a novel member of the leucine-rich repeat protein family closely related to decorin and biglycan. *J Biol Chem* 276:12201-12211.
- Murakami S, Takayama S, Kitamura M, Shimabukuro Y, Yanagi K, Ikezawa K, *et al.* (2003). Recombinant human basic fibroblast growth factor (bFGF) stimulates periodontal regeneration in class II furcation defects created in beagle dogs. *J Periodontol Res* 38:97-103.
- Nevins M, Camelo M, Nevins ML, Schenk RK, Lynch SE (2003). Periodontal regeneration in humans using recombinant human platelet-derived growth factor-BB (rhPDGF-BB) and allogenic bone. *J Periodontol* 74:1282-1292.
- Rifkin DB, Moscatelli D (1989). Recent developments in the cell biology of basic fibroblast growth factor. *J Cell Biol* 109:1-6.
- Shimabukuro Y, Ichikawa T, Takayama S, Yamada S, Takedachi M, Terakura M, *et al.* (2005). Fibroblast growth factor-2 regulates the synthesis of hyaluronan by human periodontal ligament cells. *J Cell Physiol* 203:557-563.
- Takayama S, Murakami S, Miki Y, Ikezawa K, Tasaka S, Terashima A, *et al.* (1997). Effects of basic fibroblast growth factor on human periodontal ligament cells. *J Periodontol Res* 32:667-675.
- Takayama S, Murakami S, Shimabukuro Y, Kitamura M, Okada H (2001). Periodontal regeneration by FGF-2 (bFGF) in primate models. *J Dent Res* 80:2075-2079.
- Waddington RJ, Embery G (2001). Proteoglycans and orthodontic tooth movement. *J Orthod* 28:281-290.
- Yamada S, Murakami S, Matoba R, Ozawa Y, Yokokoji T, Nakahira Y, *et al.* (2001). Expression profile of active genes in human periodontal ligament and isolation of *PLAP-1*, a novel SLRP family gene. *Gene* 275:279-286.
- Zhao M, Xiao G, Berry JE, Franceschi RT, Reddi A, Somerman MJ (2002). Bone morphogenetic protein 2 induces dental follicle cells to differentiate toward a cementoblast/osteoblast phenotype. *J Bone Miner Res* 17:1441-1451.

# Menstrual Blood-derived Cells Confer Human Dystrophin Expression in the Murine Model of Duchenne Muscular Dystrophy via Cell Fusion and Myogenic Transdifferentiation<sup>□</sup>

ChangHao Cui,<sup>\*†</sup> Taro Uyama,<sup>\*</sup> Kenji Miyado,<sup>\*</sup> Masanori Terai,<sup>\*</sup> Satoru Kyo,<sup>‡</sup> Tohru Kiyono,<sup>§</sup> and Akihiro Umezawa<sup>\*</sup>

<sup>\*</sup>Department of Reproductive Biology and Pathology, National Institute for Child Health and Development, Tokyo, 157-8567, Japan; <sup>†</sup>Department of Basic Medical Science, Mudanjiang Medical College, Mudanjiang, 157011, China; <sup>‡</sup>Department of Obstetrics and Gynecology, Kanazawa University, School of Medicine, Kanazawa, 920-8640, Japan; and <sup>§</sup>Virology Division, National Cancer Center Research Institute, Tokyo, 104-0045, Japan

Submitted September 28, 2006; Revised January 19, 2007; Accepted February 6, 2007  
Monitoring Editor: M. Bishr Omary

AQ:1

Duchenne muscular dystrophy (DMD), the most common lethal genetic disorder in children, is an X-linked recessive muscle disease characterized by the absence of dystrophin at the sarcolemma of muscle fibers. We examined a putative endometrial progenitor obtained from endometrial tissue samples to determine whether these cells repair muscular degeneration in a murine mdx model of DMD. Implanted cells conferred human dystrophin in degenerated muscle of immunodeficient mdx mice. We then examined menstrual blood-derived cells to determine whether primarily cultured nontransformed cells also repair dystrophied muscle. In vivo transfer of menstrual blood-derived cells into dystrophic muscles of immunodeficient mdx mice restored sarcolemmal expression of dystrophin. Labeling of implanted cells with EGFP and differential staining of human and murine nuclei suggest that human dystrophin expression is due to cell fusion between host myocytes and implanted cells. In vitro analysis revealed that endometrial progenitor cells and menstrual blood-derived cells can efficiently transdifferentiate into myoblasts/myocytes, fuse to C2C12 murine myoblasts by in vitro coculturing, and start to express dystrophin after fusion. These results demonstrate that the endometrial progenitor cells and menstrual blood-derived cells can transfer dystrophin into dystrophied myocytes at a high frequency through cell fusion and transdifferentiation in vitro and in vivo.

## INTRODUCTION

Skeletal muscle consists predominantly of syncytial fibers with peripheral, postmitotic myonuclei, and its intrinsic repair potential in adulthood relies on the persistence of a resident reserve population of undifferentiated mononuclear cells, termed "satellite cells." In mature skeletal muscle, most satellite cells are quiescent and are activated in response to environmental cues, such as injury, to mediate postnatal muscle regeneration. After division, satellite cell progeny, termed myoblasts, undergo terminal differentiation and become incorporated into muscle fibers (Bischoff, 1994). Myogenesis is regulated by a family of myogenic transcription factors including MyoD, Myf5, myogenin, and MRF4 (Sabourin and Rudnicki, 2000). During embryonic development, MyoD and Myf5 are involved in the establishment of the skeletal muscle lineage (Rudnicki *et al.*, 1993), whereas myogenin is required for terminal differentiation (Hasty *et al.*, 1993; Nabeshima *et al.*, 1993). During muscle

repair, satellite cells recapitulate the expression program of the myogenic genes manifested during embryonic development.

Dystrophin is associated with a large oligomeric complex of glycoproteins that provide linkage to the extracellular membrane (Ervasti and Campbell, 1991). In Duchenne muscular dystrophy (DMD), the absence of dystrophin results in destabilization of the extracellular membrane-sarcolemma-cytoskeleton architecture, making muscle fibers susceptible to contraction-associated mechanical stress and degeneration. In the first phase of the disease, new muscle fibers are formed by satellite cells. After depletion of the satellite cell pool in childhood, skeletal muscles degenerate progressively and irreversibly and are replaced by fibrotic tissue (Cossu and Mavilio, 2000). Like DMD patients, the mdx mouse lacks dystrophin in skeletal muscle fibers (Hoffman *et al.*, 1987; Sicinski *et al.*, 1989). However, the mdx mouse develops only a mild dystrophic phenotype, probably because muscle regeneration by satellite cells is efficient for most of the animal's life span (Cossu and Mavilio, 2000).

Myoblasts represent the natural first choice in cellular therapeutics for skeletal muscle because of their intrinsic myogenic commitment (Grounds *et al.*, 2002). However, myoblasts recovered from muscular biopsies are poorly expandable in vitro and rapidly undergo senescence (Cossu and Mavilio, 2000). An alternative source of muscle progenitor cells is therefore desirable. Cells with a myogenic potential are present in many tissues, and these cells readily

This article was published online ahead of print in *MBC in Press* (<http://www.molbiolcell.org/cgi/doi/10.1091/mbc.E06-09-0872>) on February 21, 2007.

□ The online version of this article contains supplemental material at *MBC Online* (<http://www.molbiolcell.org>).

Address correspondence to: Akihiro Umezawa (omezawa@1985.jukuin.keio.ac.jp).

C. Cui *et al.*

form skeletal muscle in culture (Gerhart *et al.*, 2001). We report here that human dystrophin expression in the mdx model of DMD is attributed to cell fusion of mdx myocytes with human menstrual blood-derived stromal cells.

## MATERIALS AND METHODS

### Isolation of Human Endometrial Cells from Menstrual Blood

Menstrual blood samples ( $n = 21$ ) were collected in DMEM with antibiotics (final concentrations: 100 U/ml penicillin/streptomycin) and 2% fetal bovine serum (FBS), and processed within 24 h. Ethical approval for tissue collection was granted by the Institutional Review Board of the National Research Institute for Child Health and Development, Japan. The centrifuged pellets containing endometrium-derived cells were resuspended in high-glucose DMEM medium (10% FBS, penicillin/streptomycin), maintained at 37°C in a humidified atmosphere containing 5% CO<sub>2</sub>, and allowed to attach for 48 h. Nonadherent cells were removed by changing the medium. When the culture reached subconfluence, the cells were harvested with 0.25% trypsin and 1 mM EDTA and plated to new dishes. After 2–3 passages, the attached endometrial stromal cells were devoid of blood cells. Human EM-E6/E7/hTERT-2 cells, endometrium-derived progenitors, were obtained from surgical endometrial tissue samples and were immortalized by E6, E7, and hTERT-2 (Kyo *et al.*, 2003). C2C12 myoblast cells were supplied by RIKEN Cell Bank (The Institute of Physical and Chemical Research, Japan).

### Flow Cytometric Analysis

Flow cytometric analysis was performed as previously described (Terai *et al.*, 2005). Cells were incubated with primary antibodies or isotype-matched control antibodies, followed by additional treatment with the immunofluorescent secondary antibodies. Cells were analyzed on an EPICS ALTRA analyzer (Beckman Coulter, Fullerton, CA). Antibodies against human CD13, CD14, CD29, CD31, CD34, CD44, CD45, CD50, CD54, CD55, CD59, CD73, CD90, CD105, CD117 (c-kit), CD133, HLA-ABC, and HLA-DR were purchased from Beckman Coulter, Immunotech (Marseille, France), Cytotech (Hellebaek, Denmark), and BD Biosciences Pharmingen (San Diego, CA).

### In Vitro Lentivirus-mediated Gene (EGFP) Transfer into EM-E6/E7/hTERT-2 Cells

infection of EM-E6/E7/hTERT-2 cells with lentivirus having a CMV promoter and EGFP reporter resulted in high levels of EGFP expression in all cells. Cells were analyzed for EGFP expression by flow cytometry (Miyoshi *et al.*, 1997, 1998).

### In Vitro Myogenesis

Menstrual blood-derived cells or EM-E6/E7/hTERT-2 cells were seeded onto collagen I-coated cell culture dishes (Biocoat, BD Biosciences, Bedford, MA) at a density of  $1 \times 10^4$ /ml in growth medium (DMEM, supplemented with 20% FBS). Forty-eight hours after seeding onto collagen I-coated dishes, cells were treated with 5-azacytidine for 24 h. Cell cultures were then washed twice with PBS and maintained in differentiation medium (DMEM, supplemented with either 2% horse serum (HS) or 1% insulin-transferrin-selenium supplement [ITS]). The differentiation medium was changed twice a week until the experiment was terminated.

### RT-PCR Analysis of EM-E6/E7/hTERT-2 Cells and Menstrual Blood-derived Cells

Total RNA was prepared using Isogen (Nippon Gene, Tokyo, Japan). Human skeletal muscle RNA was purchased from TOYOBO (Osaka, Japan). RT-PCR of Myf5, MyoD, desmin, myogenin, myosin heavy chain-IIx/d (MyHC-IIx/d), and dystrophin was performed with 2  $\mu$ g of total RNA. RNA for RT-PCR was converted to cDNA with a first-stand cDNA synthesis kit (Amersham Pharmacia Biotechnology, Piscataway, NJ) according to the manufacturer's recommendations. The sequences of PCR primers that amplify human but not mouse genes are listed in Supplementary Table 1. PCR was performed with TaKaRa recombinant Taq (Takara Shuzo, Kyoto, Japan) for 30 cycles, with each cycle consisting of 94°C for 30 s, 62°C or 65°C for 30 s, and 72°C for 20 s, with an additional 10-min incubation at 72°C after completion of the last cycle.

### Immunohistochemical and Immunocytochemical Analysis

Immunohistochemical analysis was performed as previously described (Mori *et al.*, 2005). Briefly, the sections were incubated for 1 h at room temperature with mouse mAb against vimentin (Cone V9, DakoCytomation, Fort Collins, CO). After washing in PBS, sections were incubated with horseradish peroxidase-conjugated rabbit anti-mouse immunoglobulin, diluted, and washed in cold PBS. Staining was developed by using a solution containing diaminobenzidine and 0.01% H<sub>2</sub>O<sub>2</sub> in 0.05% M Tris-HCl buffer, pH 6.7. Slides were

counterstained with hematoxylin. In the cases of fluorescence, frozen sections fixed with 4% PFA were used. The antibodies against human dystrophin (NCL-DYS3; Novocastra, Newcastle upon Tyne, United Kingdom) or anti-human nuclei mouse mAb (clone 235-1, Chemicon, Temecula, CA) was used as a first antibody, and goat anti-mouse IgG conjugated with Alexa Fluor 488 or goat anti-mouse IgG antibody conjugated with Alexa Fluor 546 (Molecular Probes, Eugene, OR) was used as a second antibody.

Immunocytochemical analysis was performed as previously described (Mori *et al.*, 2005), with antibodies to skeletal myosin (Sigma, St. Louis, MO; product no. M 4276), MF20 (which reacts with all sarcomere myosin in striated muscles, Developmental Studies Hybridoma Bank, University of Iowa, IA),  $\alpha$ -sarcomeric actin (Sigma, product no. A 7811), and desmin (BioScience Products, Bern, Switzerland; no. 010031, clone: D9) in PBS containing 1% bovine serum albumin. As a methodological control, the primary antibody was omitted. In the cases of fluorescence, slides were incubated with Alexa Fluor 546-conjugated goat anti-mouse IgG antibody.

### Western Blotting

Western blot analysis was performed as previously described (Mori *et al.*, 2005). Blots were incubated with primary antibodies (desmin, myogenin [Clone F5D, Santa Cruz Biotechnology], and dystrophin [NCL-DYSA, Novocastra]) for 1–2 h at room temperature. After washing three times in the blocking buffer, blots were incubated for 30 min with a horseradish peroxidase-conjugated secondary antibody (0.04  $\mu$ g/ml) directed against the primary antibody. The blots were developed with enhanced chemiluminescence substrate according to the manufacturer's instructions.

### Fusion Assay

EM-E6/E7/hTERT-2 cells (2500/cm<sup>2</sup>) or EGFP-labeled EM-E6/E7/hTERT-2 cells (2500/cm<sup>2</sup>) were cocultured with C2C12 myoblasts (2500/cm<sup>2</sup>) for 2 d in DMEM supplemented with 10% FBS and then cultured for 7 additional days in DMEM with 2% HS to promote myotube formation. The cultures were fixed in 4% paraformaldehyde and stained with a mouse anti-human nuclei IgG1 mAb and the mouse anti-human dystrophin IgG2a mAb (or anti-myosin heavy chain IgG2b mAb MF-20). The cells were visualized with appropriate Alexa-fluor-conjugated goat anti-mouse IgG1 and IgG2a (or IgG2b) secondary antibodies (Molecular Probes). Total cell nuclei were stained with DAPI (4',6-diamidino-2-phenylindole).

### In Vivo Cell Implantation

Six- to 8-wk-old NOD/Shi-scid/IL-2 receptor  $-/-$  (NOG, CREA, Shizuoka, Japan) mice and 6- to 8-wk-old mdx-scid mice were implanted with EM-E6/E7/hTERT-2 cells and menstrual blood-derived cells in seven independent experiments. The cells ( $2 \times 10^7$ ) were suspended in PBS in a total volume of 100  $\mu$ l and were directly injected into the right thigh muscle of NOG mice or mdx-scid mice. The mice were examined 3 wk after cell implantation, and the right thigh muscle was analyzed for human vimentin and dystrophin by immunohistochemistry. The antibodies to vimentin and dystrophin (NCL-DYS3) react with human vimentin and dystrophin-equivalent protein, but not murine protein.

## RESULTS

### Surface Marker Expression of Endometrium-derived Cells

We investigated myogenic differentiation of primary cells without gene introduction from menstrual blood, because menstrual blood on the first day of the period is considered to include endometrial tissue. We successfully cultured a large number of primary cells from menstrual blood. Menstrual blood-derived cells showed at least two morphologically different cell groups: small spindle-like cells and large stick-like cells, regarded as being passage day (PD) 1 or 2 (Figure 1, A and B, respectively). Surface markers of the menstrual blood-derived cells were evaluated by flow cytometric analysis. Surface markers of EM-E6/E7/hTERT-2 cells (Figure 1C) and menstrual blood-derived cells (Figure 1D) were evaluated by flow cytometric analysis (Figure 1E). In these experiments, the cells were cultured in the absence of any inductive stimuli. EM-E6/E7/hTERT-2 cells were positive for CD13, CD29 (integrin  $\beta$ 1), CD44 (Pgp-1/ly24), CD54, CD55, CD59, CD73, and CD90 (Thy-1), implying that EM-E6/E7/hTERT-2 cells expressed mesenchymal cell-related antigens in our experimental setting. Menstrual blood-derived cells were positive for CD13, CD29, CD44, CD54, CD55, CD59, CD73, CD90, and CD105, implying that prolif-

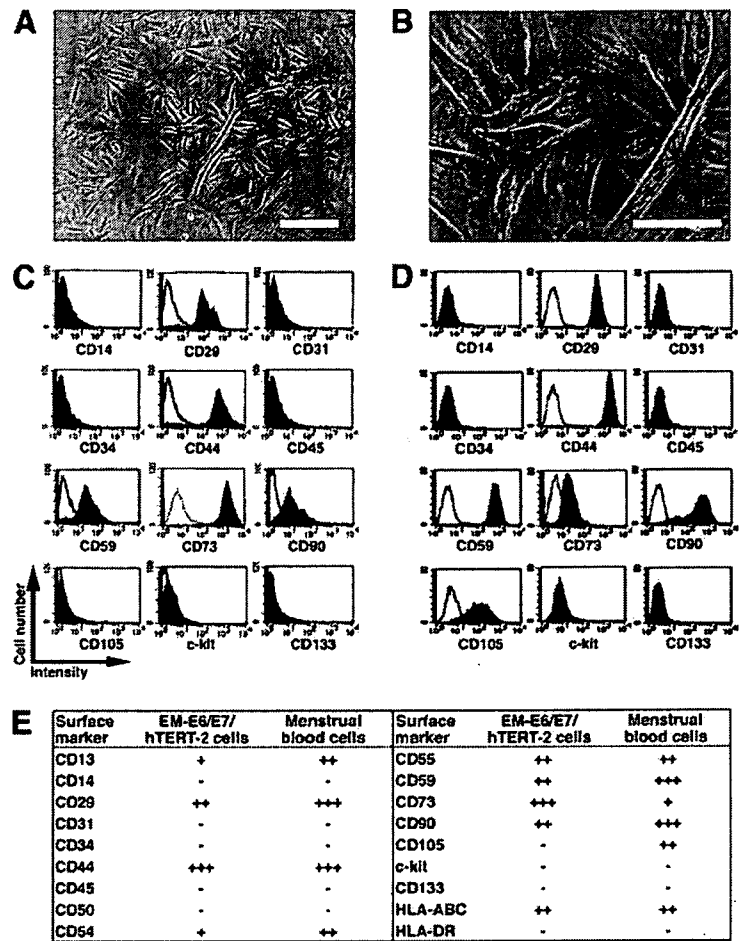


**Figure 1.** Surface marker expression of endometrium-derived cells. (A and B) Morphology of menstrual blood-derived cells, regarded as being PD 1 or 2. Scale bars, 200  $\mu\text{m}$  (A), 100  $\mu\text{m}$  (B). (C and D) Flow cytometric analysis of cell surface markers of EM-E6/E7/hTERT-2 cells (C) and menstrual blood-derived cells (D). (E) Further phenotypic analysis in EM-E6/E7/hTERT-2 cells and menstrual blood-derived cells are summarized. Peak intensity was estimated in comparison with isotype controls. +++, strongly positive (>100 times the isotype control); ++, moderately positive (<100 times but more than 10 times the isotype control), weakly positive (<10 times but more than twice the isotype control), -, negative (less than twice the isotype control).

erated and propagated cells express mesenchymal cell-related cell surface markers. Unlike EM-E6/E7/hTERT-2 cells, the menstrual blood-derived adherent cells were positive for CD105. EM-E6/E7/hTERT-2 cells and menstrual blood-derived cells expressed neither hematopoietic lineage markers, such as CD34, nor monocyte-macrophage antigens such as CD14 (a marker for macrophage and dendritic cells), or CD45 (leukocyte common antigen). The lack of expression of CD14, CD34, or CD45 suggests that EM-E6/E7/hTERT-2 cells and the menstrual blood-derived cell culture in the present study is depleted of hematopoietic cells. The cells were also negative for expression of CD31 (PECAM-1), CD50, c-kit, and CD133. The cell population was positive for HLA-ABC, but not for HLA-DR. These results demonstrate that almost all cells derived from endometrium are of mesenchymal origin or stromal origin.

**Implanted Endometrium-derived Cells Induce De Novo Myogenesis in Immunodeficient NOG Mice**

EM-E6/E7/hTERT-2 cells originate from the endometrial gland and are considered as endometrial progenitor cells or bipotential cells capable of differentiating into both glandular epithelial cells and endometrial stromal cells (Kyo *et al.*, 2003). To determine whether EM-E6/E7/hTERT-2 cells and menstrual blood-derived cells generate complete endometrial structure *in vivo*, like endometriosis, the cells without any treatment or induction were injected into the right thigh

muscle of immunodeficient NOG mice. PBS without cells was injected into the left thigh muscles as a control. We failed to detect any endometrial structure in the cell-injected site. Immunohistochemical analysis using an antibody specific to human vimentin, an intermediate filament associated with a mesenchymal cell, revealed that the injected EM-E6/E7/hTERT-2 cells (Figure 2, A-F) or menstrual blood-derived cells (Figure 2, G-L) extensively migrated or infiltrated between muscular fibers (Figure 2, arrowheads). To investigate if the donor cells between muscular fibers occur as a result of cell migration, we performed a time-course analysis of implanted cells, as probed by human-specific antibody to vimentin (Supplementary Figure 1). Donor cells at 3 h after implantation are observed at the injection site, which is considered to be due to just injection of cells. Cells at 1-3 wk after implantation are detected between myocytes in the muscle bundle or muscular fascicle as well as in the interstitial tissue, implying that the donor cells between myotubes result from cell migration. Interestingly, some of the vimentin-positive implanted cells exhibited round-shaped structure (Figure 2, D, F, and J, arrows), suggesting that endometrium-derived cells are capable of differentiating into myoblasts/myotubes, and can contribute to skeletal muscle repair in patients suffering from genetic disorders such as DMD, similar to previous reports for marrow stromal cells (Dezawa *et al.*, 2005) and synovial membrane cells (De Bari *et al.*, 2003).



C. Cui et al.

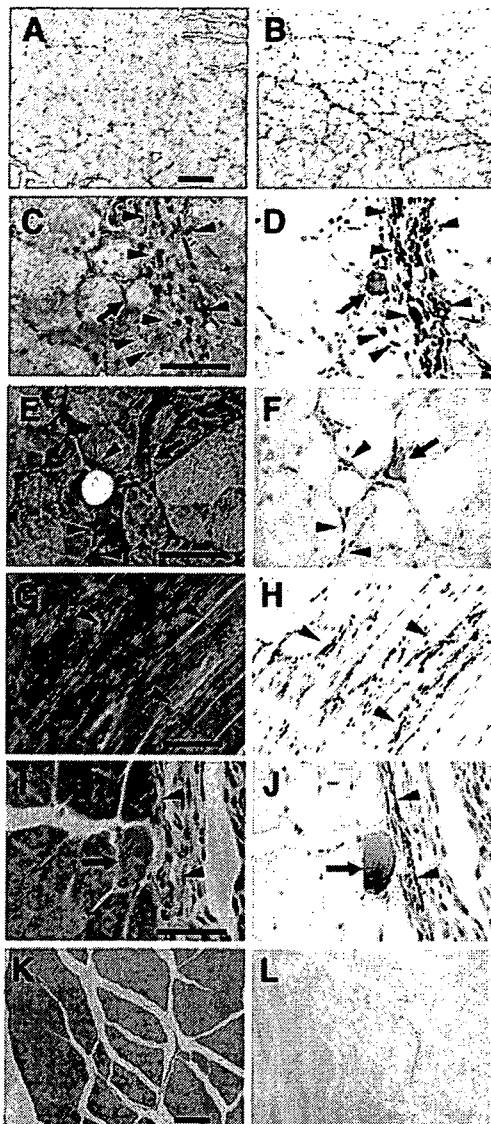


**Figure 2.** Implantation of endometrium-derived cells into the muscle of NOG mice. EM-E6/E7/hTERT-2 cells (A–F) or menstrual blood-derived cells (G–J) cultured in absence of any stimuli were directly injected into the right thigh muscle of NOG mice. Immunohistochemical analysis was performed using antibody that reacts to human vimentin but not to murine vimentin. (A, C, E, G, I, and K) hematoxylin and eosin stain (HE; B, D, F, H, J, and L) immunohistochemistry. Note that vimentin-positive EM-E6/E7/hTERT-2 cells and menstrual blood-derived cells with a spindle morphology (C–J, arrowheads) extensively migrated into muscular bundles at 3 wk after injection, and some of the injected cells exhibited round structure (D, F, and J, arrows). Isotype mouse IgG1 served as a negative control (L). Scale bars, 100  $\mu$ m (A, B, K, and L), 50  $\mu$ m (C–F, I, and J), 90  $\mu$ m (G and H).

### Induction of Myogenic Differentiation in Endometrial Progenitor Cells In Vitro

EM-E6/E7/hTERT-2 cells at 2 wk (cultured in the DMEM supplemented with 20% FBS) after exposure to different concentrations (5, 10, and 100  $\mu$ M) of 5-azacytidine were analyzed by immunostaining using anti-desmin antibody (Figure 3, A–F). The number of desmin-positive cells was

significantly higher in experimental groups with 5 or 10  $\mu$ M 5-azacytidine than in untreated control groups ( $p < 0.05$ ). To investigate whether EM-E6/E7/hTERT-2 cells are capable of differentiating into skeletal muscle cells in vitro, the cells were exposed to 5  $\mu$ M 5-azacytidine for 24 h and then subsequently cultured in the DMEM supplemented with 2% HS (Figure 3, G–J) or serum-free ITS for up to 21 d (Figure 3K). Skeletal myoblastic differentiation of the cells was analyzed by evaluating expression of MyoD, Myf5, desmin, myogenin, MyHC-IIx/d, and dystrophin by RT-PCR. The MyoD, desmin, myogenin, and dystrophin genes were constitutively expressed, but MyHC-IIx/d and Myf5 genes were not. The decline of MyoD was observed in both the 2% HS (Figure 3, G and H) and the serum-free ITS (Figure 3K). The expression of MyHC, as determined by RT-PCR and immunocytochemistry, significantly increased with 2% HS (Figure 3, G–J) and serum-free ITS (Figure 3K). Immunocytochemical analysis indicated that  $\alpha$ -sarcomeric actin (Figure 3I) and MyHC (Figure 3J) were detected in the cells incubated with 2% HS for 21 d.

### In Vitro Myogenic Differentiation of Menstrual Blood-derived Cells

Menstrual blood-derived cells at 3 wk (cultured in DMEM supplemented with 20% FBS) after exposure to different concentrations (5, 10, and 100  $\mu$ M) of 5-azacytidine were analyzed by immunostaining using anti-desmin antibody (data not shown). The number of desmin-positive cells was significantly higher in experimental groups with 5 or 10  $\mu$ M 5-azacytidine than with 100  $\mu$ M 5-azacytidine; for further in vitro experiments, the menstrual blood-derived cells were exposed to 5  $\mu$ M 5-azacytidine for 24 h and then subsequently cultured in DMEM supplemented with low serum (2% HS) or serum-free ITS for up to 21 d (Figure 4). Myogenic potential of human menstrual blood-derived cells was analyzed by evaluating the expression of Myf5, MyoD, desmin, myogenin, MyHC-IIx/d, and dystrophin by RT-PCR. MyoD, desmin, and dystrophin genes were constitutively expressed in menstrual blood-derived cells, but MyHC-IIx/d and Myf5 were not (Figure 4A). For cells treated with 2% HS or serum-free ITS, the mRNA level of desmin and myogenin significantly increased after 3 d, and desmin steadily increased until day 21 (Figure 4, C and D). MyHC-IIx/d started to be expressed at a low level at day 21 of induction (Figure 4C). We then analyzed desmin expression by immunocytochemistry. Menstrual blood-derived cells were exposed to 5  $\mu$ M 5-azacytidine for 24 h and then subsequently cultured in DMEM supplemented with 20% FBS for up to 2 wk. Desmin was readily detected in colonies of the menstrual blood-derived cells (Figure 4B). Western blot analysis indicated that desmin, myogenin, and dystrophin were highly expressed in the cells incubated for 3 wk (Figure 4, E–G). These results suggest that menstrual blood-derived cells are, like the EM-E6/E7/hTERT-2 cells, able to differentiate into skeletal muscle.

### Regeneration of Dystrophin by Cell Implantation in the DMD Model *mdx-scid* Mouse

To investigate whether human EM-E6/E7/hTERT-2 cells and menstrual blood-derived cells can generate muscle tissue in vivo, cells without any treatment or induction were implanted directly into the right thigh muscles of *mdx-scid* mice (Supplementary Figure 2). The left thigh muscles were injected with PBS as an internal control. After 3 wk, myotubes in the muscle tissues injected with human EM-E6/E7/hTERT-2 cells and menstrual blood-derived cells expressed human dystrophin as a cluster (Figure 5, A, C, and D, EM-

F3, AQ:5

F4, AQ:6

F5



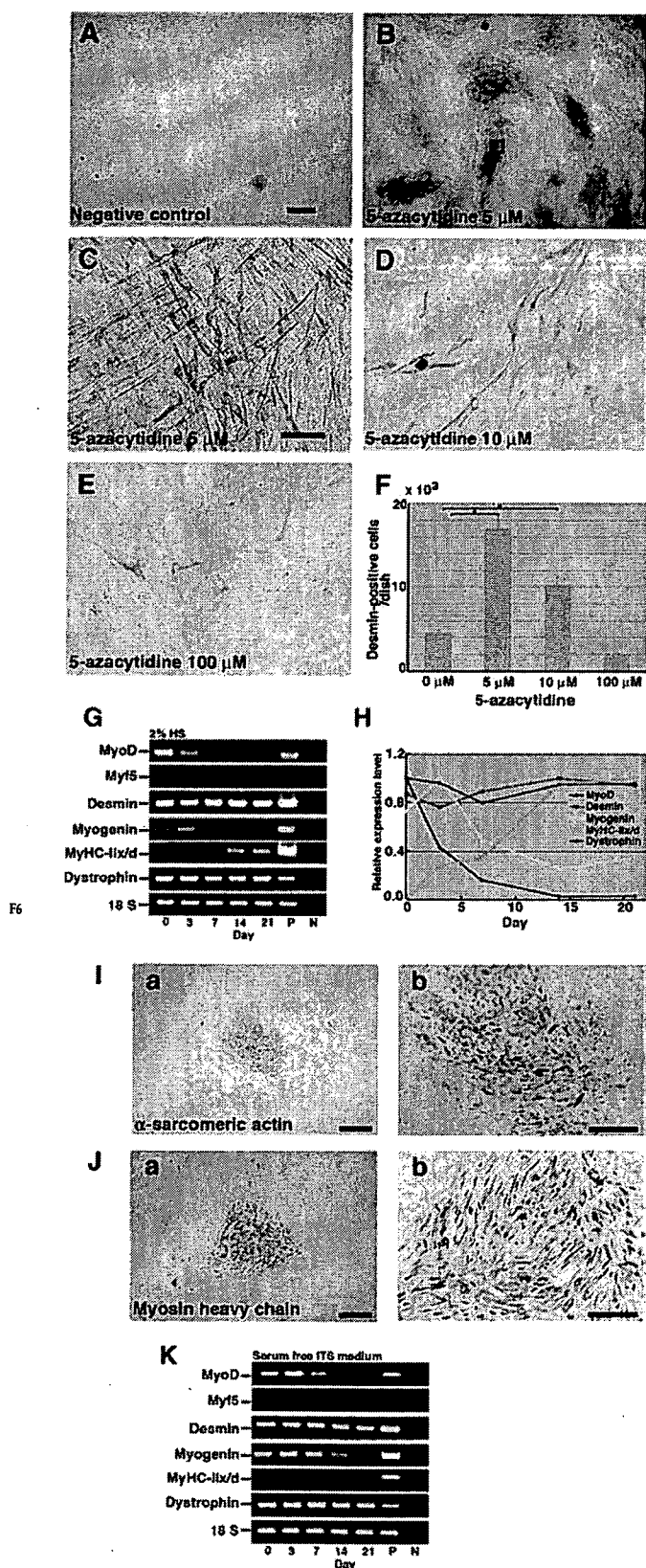


Figure 3. Expression of myogenic-specific genes during myogenic differentiation of EM-E6/E7/hTERT-2 cells. (A-F) Immunocytochemical

E6/E7/hTERT-2 cells, and 5B, menstrual blood-derived cells). Quantification analysis revealed that the percentage of dystrophin-positive myofibers after implantation of menstrual blood-derived cells was high, compared with that after implantation of EM-E6/E7/hTERT-2 cells (Figure 5E). Donor cells with EGFP fluorescence participated in myogenesis 3 wk after implantation (Supplementary Figure 3). EGFP-labeled EM-E6/E7/hTERT-2 cells became positive for human dystrophin (Figure 5C). Dystrophin was not detected in the muscle of mdx-scid mice and NOG mice without cell implantation because the antibody to dystrophin used in this study is human-specific, implying that dystrophin expression is attributed to fusion between murine host myocytes and human donor cells, rather than myogenic differentiation of EM-E6/E7/hTERT-2 cells and menstrual blood-derived cells per se.

To determine if dystrophin expression in the donor cells is due to transdifferentiation or fusion, immunohistochemistry with an antibody against human nuclei (Ab-HuNucl) and DAPI stain was performed. If dystrophin expression is explained by fusion, dystrophin-positive myocytes must be demonstrated to have both human and murine nuclei. We examined almost all the 7- $\mu$ m-thick serial histological sections parallel to the muscular bundle (longitudinal section) of the muscular tissues by confocal microscopy and found that dystrophin-positive myocytes have nuclei derived from both human and murine cells in the longitudinal section of the myocytes (Figure 5D), implying that dystrophin expression is attributed to fusion between murine host myocytes and human donor cells, rather than myogenic differentiation of EM-E6/E7/hTERT-2 cells and menstrual blood-derived cells per se.

**Detection of Human Endometrial Cell Contribution to Myotubes in an In Vitro Myogenesis Model**

To simulate in vivo phenomena, human endometrial cells were cocultured in vitro with murine C2C12 myoblasts for 2 d under proliferative conditions and then switched to differentiation conditions for an additional 7 d. Figure 6A

analysis of EM-E6/E7/hTERT-2 cells using an antibody to desmin. (A) Omission of only the primary antibody to desmin serves as a negative control. (B) Higher magnification of inset in B. (F) Myogenic differentiation of EM-E6/E7/hTERT-2 cells with exposure to different concentrations (B, 5  $\mu$ M; C, 5  $\mu$ M; D, 10  $\mu$ M, E, 100  $\mu$ M) of 5-azacytidine. To estimate myogenic differentiation, the number of all the desmin-positive cells was counted for each dish (n = 3). Data were analyzed for statistical significance using ANOVA. EM-E6/E7/hTERT-2 cells were cultured in the DMEM supplemented with 2% HS (G-J; horse serum), and serum-free ITS (K). (G and K) RT-PCR analysis with PCR primers allows amplification of the human MyoD, Myf5, desmin, myogenin, myosin heavy chain type IIx/d (MyHC-IIx/d), and dystrophin cDNA (from top to bottom). RNAs were isolated from EM-E6/E7/hTERT-2 cells at the indicated day after treatment with 5-azacytidine. RNAs from human muscle and H<sub>2</sub>O served as positive (P) and negative (N) controls. Only the 18S PCR primer used as a positive control reacted with the human and murine cDNA. (H) Time course of MyoD, desmin, myogenin, MyHC-IIx/d, and dystrophin expression in the cells incubated with 2% HS for up to 21 d after 5-azacytidine treatment. Relative mRNA levels were determined using Multi Gauge Ver 2.0 (Fuji Film). The signal intensities of MyoD, desmin, and dystrophin mRNA at day 0, myogenin mRNA at day 3, and MyHC-II/d mRNA at day 21 were regarded as equal to 100%. (I and J) The cells were exposed to 5  $\mu$ M 5-azacytidine for 24 h and then subsequently cultured in DMEM supplemented with 2% HS for 21 d.  $\alpha$ -Sarcomeric actin (I) and skeletal myosin heavy chain (J) was detected by immunocytochemical analysis. Scale bars, 2 mm (A and B), 300  $\mu$ m (C-E), 900  $\mu$ m (Ia and Ja), 425  $\mu$ m (Ib and Jb).

C. Cui *et al.*

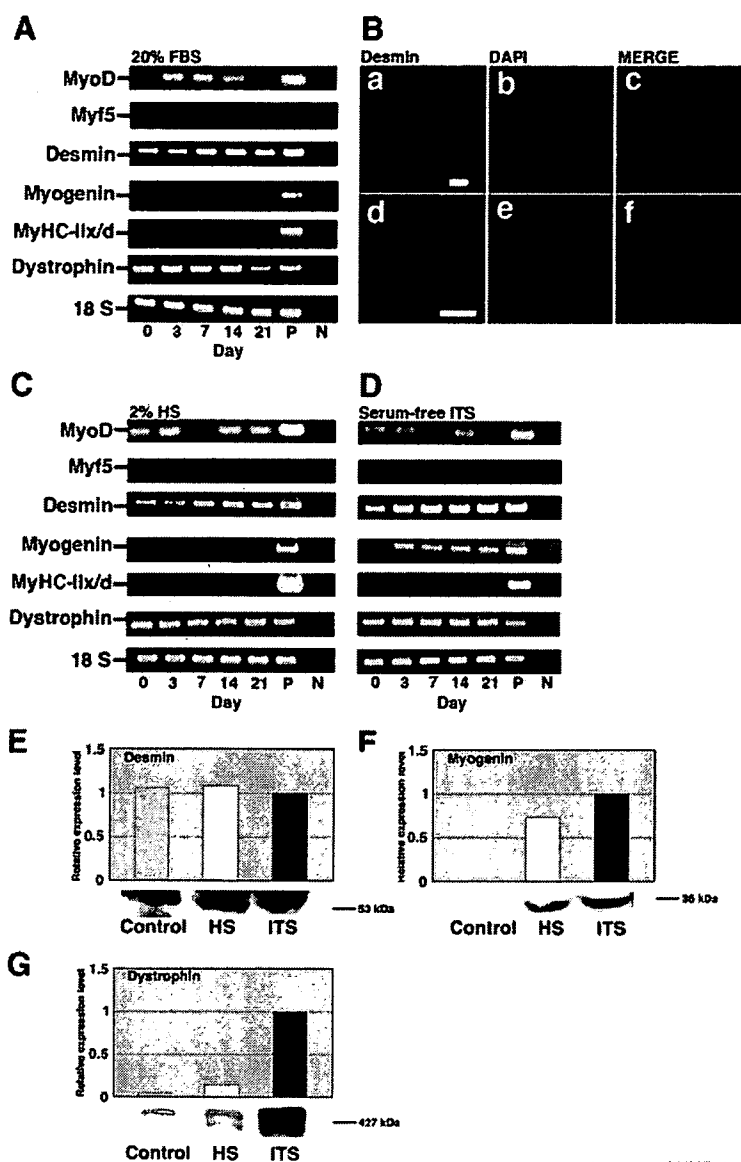


**Figure 4.** Expression of myogenic-specific genes in differentiated menstrual blood-derived cells. Menstrual blood-derived cells were cultured in DMEM supplemented with 20% FBS, 2% HS, or serum-free ITS medium. (A) RT-PCR analysis with PCR primers that allows amplification of the human MyoD, Myf5, desmin, myogenin, MyHC-IIx/d, and dystrophin cDNA (from top to bottom). RNAs were isolated from menstrual blood-derived cells at the indicated day after treatment with 5  $\mu$ M 5-azacytidine for 24 h. RNAs from human muscle and H<sub>2</sub>O served as positive (P) and negative (N) controls. Only the 18S PCR primer used as a positive control reacted with the human and murine cDNA. (B) Immunocytochemical analysis using an antibody to desmin (a–f) was performed on the menstrual blood-derived cells at 2 wk after exposure to 5  $\mu$ M of 5-azacytidine for 24 h. The desmin-positive cells are shown at higher magnification (d–f). Merge of a and b is shown in c, and merge of d and e is shown in f. The images were obtained with a laser scanning confocal microscope. Scale bars, 200  $\mu$ m (a–c) and 75  $\mu$ m (d–f). (C and D) RT-PCR analysis of menstrual blood-derived cells on DMEM supplemented with 2% HS (C) or serum-free ITS medium (D) after exposure to 5  $\mu$ M 5-azacytidine for 24 h. (E–G) Western blot analysis was performed on the cells cultured in myogenic medium indicated for 21 d. The blot was stained with desmin (E), myogenin (F), and dystrophin (G) antibodies followed by an HRP-conjugated secondary antibody.

provides an example of how human and mouse nuclei in the EGFP-positive myotubes were detected. Multinucleated myotubes were revealed by the presence of specific human dystrophin (Figure 6, B and C) and myosin heavy chain (Figure 6D). Dystrophin was detected in cytoplasm in culture condition (Figure 6, B and C) despite evidence of cell surface localization in vivo. Human dystrophin and human nuclei were unequivocally identified by staining with antibodies to human dystrophin and human nuclei, whereas the numerous mouse nuclei present in this field, as shown by DAPI staining, are negative (Figure 6, B and C).

## DISCUSSION

Skeletal muscle has a remarkable regenerative capacity in response to an extensive injury. Resident within adult skeletal muscle is a small population of myogenic precursor cells (or satellite cells) that are capable of multiple rounds of proliferation (estimated at 80–100 doublings), which are

able to reestablish a quiescent pool of myogenic progenitor cells after each discrete regenerative episode (Mauro, 1961; Schultz and McCormick, 1994; Seale and Rudnicki, 2000; Hawke and Garry, 2001). Although muscle regeneration is a highly efficient and reproducible process, it ultimately is exhausted, as observed in senescent skeletal muscle or in patients with muscular dystrophy (Gussoni *et al.*, 1997; Cossu and Mavilio, 2000). In the present study, we investigated the myogenic potential of human endometrial tissue-derived immortalized EM-E6/E7/TERT-2 cells and primary cells derived from human menstrual blood. Human menstrual blood-derived cells proliferated over at least 25 PDs (9 passages) for more than 60 d and stopped dividing before 30 PDs. This cessation of cell division is probably due to replicative senescence or shortening of telomere length. Cell life span of menstrual blood cells is relatively short when compared with human fetal cells (Imai *et al.*, 1994; Terai *et al.*, 2005), and this shorter cell life span may be attributed to shorter telomere length of adult cells (i.e., endometrial stro-

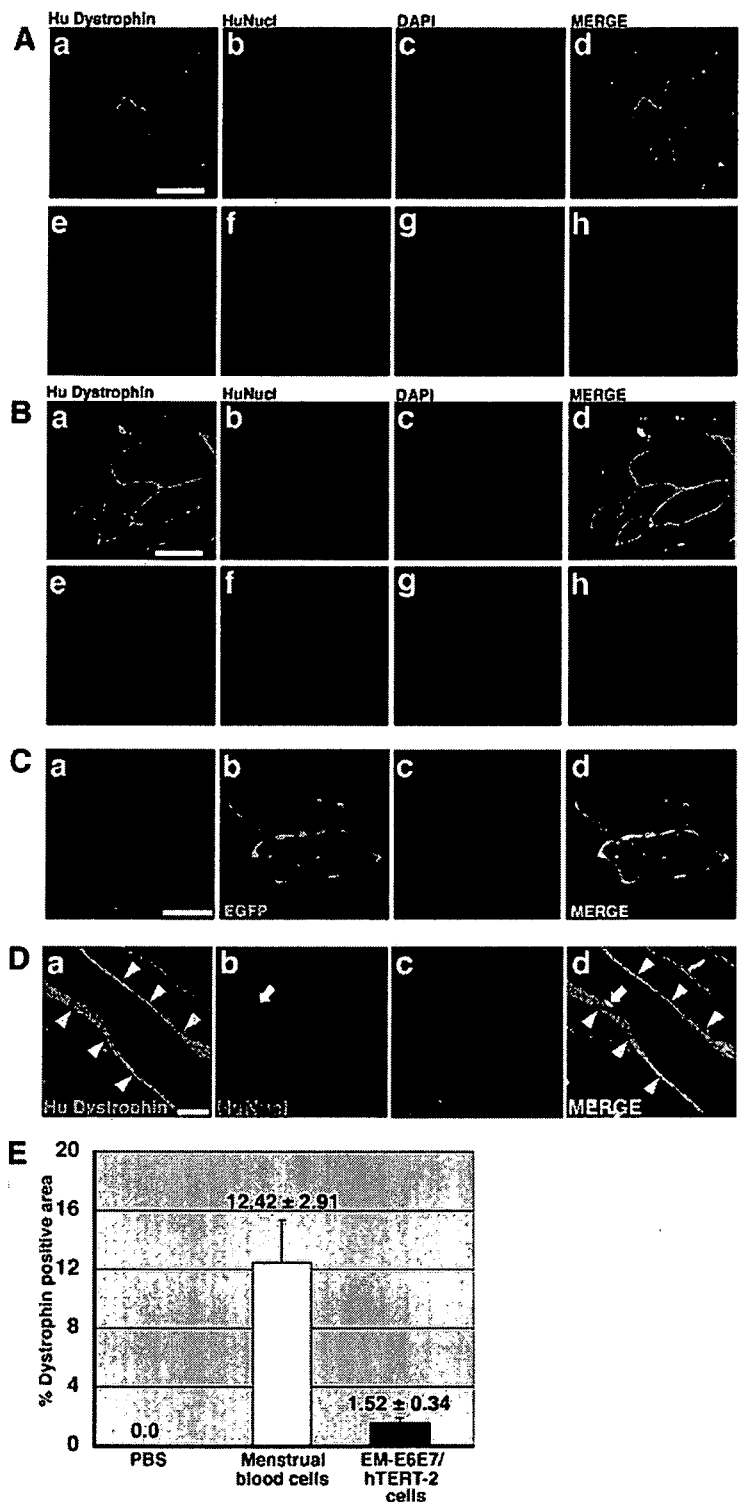


**Figure 5.** Conferral of dystrophin to mdx myocytes by human endometrial cells. (A and B) Immunohistochemistry analysis using an antibody against human dystrophin molecule (green), human nuclei (HuNucl, red), and DAPI staining (blue) on thigh muscle sections of mdx-scid mice after direct injection of EM-E6/E7/hTERT-2 cells (A) or menstrual blood-derived cells (B) without any treatment or induction. (C) EGFP-labeled EM-E6/E7/hTERT-2 cells without any treatment or induction were directly injected into the thigh muscle of mdx-scid mice. Immunohistochemistry revealed the incorporation of implanted cells into newly formed EGFP-positive myofibers, which expressed human dystrophin 3 wk after implantation. (A and B) As a methodological control, the primary antibody to dystrophin was omitted (e and f). (D) Immunohistochemistry analysis using an antibody against human dystrophin molecule (green, arrowheads), human nuclei (HuNucl, red, arrow), and DAPI staining (blue) on thigh muscle sections of mdx-scid mice after direct injection of human EM-E6/E7/hTERT-2 cells without any treatment or induction. (A and B) Merge of a-c is shown in d, and merge of e-g is shown in h. (C and D) Merge of a-c is shown in d. Scale bars, 50  $\mu$ m (A and B), 20  $\mu$ m (C and D). (E) Quantitative analysis of human dystrophin-positive myotubes. Menstrual blood-derived cells or EM-E6/E7/hTERT-2 cells without any treatment or induction were directly injected into thigh muscle of mdx-scid mice. The percentage of human dystrophin-positive-myofiber areas was calculated 3 wk after implantation of the EM-E6/E7/hTERT-2 cells or menstrual blood-derived cells. Injection of PBS without cells into mdx-scid myofibers was used as a control.

mal cells) at the start of cell cultivation, as is the case with hematopoietic stem cells (Suda *et al.*, 1984).

Menstrual blood-derived cells had a high replicative ability similar to progenitors or stem cells that display a long-term self-renewal capacity and had a much higher growth rate in our experimental conditions than marrow-derived

stromal cells (Mori *et al.*, 2005). In addition, the myogenic potential of menstrual blood-derived cells, i.e., a high frequency of desmin-positive cells after induction, is much greater than expected. The higher myogenic differentiation ratio can be explained just by alteration of cell characteristics from epithelial and mesenchymal bipotential cells or heter-

C. Cui *et al.*

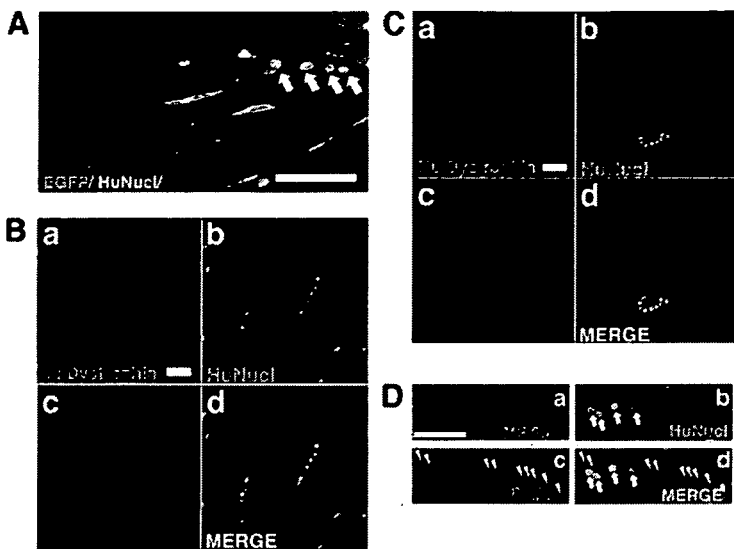


**Figure 6.** Detection of human endometrial cell contribution to myotubes in an *in vitro* and *in vivo* myogenesis model. EGFP-labeled EM-E6/E7/hTERT-2 cells (A) or EM-E6/E7/hTERT-2 cells (B) or menstrual blood-derived cells (C and D) were cocultured with C2C12 myoblasts for 2 d under conditions that favored proliferation. The cultures were then changed to differentiation media for 7 d to induce myogenic fusion. (A) Myotubes were revealed by EGFP (green); human nuclei were detected by antibody specific to human nuclei (HuNucl, red, arrows). (B–D) Myotubes were revealed by specific human dystrophin mAb NCL-DYS3 (B and C, red) or anti-myosin heavy chain mAb MF-20 (D, red). (D) Human nuclei were detected by antibody specific to human nuclei (HuNucl, green, arrows). Total cell nuclei in the culture were stained with DAPI (blue, arrowheads). (B–D) Merge of a–c are shown in d. The cultures were then changed to differentiation media for 7 d to induce myogenic fusion. Scale bars, 100  $\mu$ m (A–D).

ogeneous populations of cells to cells with the mesenchymal phenotype in our cultivation condition, as determined by cell surface markers (Figure 1, C–E). MyoD-positive cells are present in many fetal chick organs such as brain, lung, intestine, kidney, spleen, heart, and liver (Gerhart *et al.*, 2001), and these cells can differentiate into skeletal muscle in culture. Constitutive expression of MyoD, desmin, and myogenin, all markers for skeletal myogenic differentiation in both immortalized EM-E6/E7/hTERT-2 cells and menstrual blood-derived cells, implies either that most of these cells are myogenic progenitors or that these cells have myogenic potential. Expression of MyoD, one of the basic helix-loop-helix transcription factors that directly regulate myocyte cell specification and differentiation (Edmondson and Olson, 1993), occurs at the early stage of myogenic differentiation, whereas myogenin is expressed later, related to cell fusion and differentiation (Aurade *et al.*, 1994).

Acquisition or recovery of dystrophin expression in dystrophic muscle is attributed to two different mechanisms: 1) myogenic differentiation of implanted or transplanted cells and 2) cell fusion of implanted or transplanted cells with host muscle cells. Recovery of dystrophin-positive cells is explained by muscular differentiation of implanted marrow stromal cells and adipocytes (Dezawa *et al.*, 2005; Rodriguez *et al.*, 2005). In contrast, implantation of normal myoblasts into dystrophin-deficient muscle can create a reservoir of normal myoblasts that are capable of fusing with dystrophic muscle fibers and restoring dystrophin (Mendell *et al.*, 1995; Terada *et al.*, 2002; Wang *et al.*, 2003; Dezawa *et al.*, 2005; Rodriguez *et al.*, 2005). In this study using menstrual blood-derived cells, our findings—that the implantation of immortalized EM-E6/E7/hTERT-2 cells and menstrual blood-derived cells improved the efficiency of muscle regeneration and dystrophin delivery to dystrophic muscle in mice—is explained by both possibilities or the latter possibility alone, because cells expressing human dystrophin had both murine and human nuclei, located in the center and periphery of dystrophic muscular fiber, respectively (Figures 5D, *in vivo*, and 6, A–D, *in vitro*).

DMD is a devastating X-linked muscle disease characterized by progressive muscle weakness attributable to a lack of dystrophin expression at the sarcolemma of muscle fibers (Mendell *et al.*, 1995; Rodriguez *et al.*, 2005), and there are no

effective therapeutic approaches for muscular dystrophy at present. Human menstrual blood-derived cells are obtained by a simple, safe, and painless procedure and can be expanded efficiently *in vitro*. In contrast, isolation of mesenchymal stem cells/mesenchymal cells from other sources, such as bone marrow and adipose tissue, is accompanied by a painful and complicated operation. Efficient fusion systems of our immortalized human EM-E6/E7/hTERT-2 cells and menstrual blood-derived cells with host dystrophic myocytes may contribute substantially to a major advance toward eventual cell-based therapies for muscle injury or chronic muscular disease. Finally, we would like to reemphasize that human menstrual blood-derived cells possess high self-renewal capacity, whereas biopsied myoblasts capable of differentiating into muscular cells are poorly expandable *in vitro* and rapidly undergo senescence (Cossu and Mavilio, 2000).

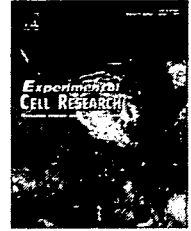
#### ACKNOWLEDGMENTS

We express our sincere thanks to J. Hata for support throughout this work, to H. Abe for providing expert technical assistance, to K. Saito for secretarial work, and to A. Crump for reviewing the manuscript. This study was supported by grants from the Ministry of Education, Culture, Sports, Science, and Technology (MEXT) of Japan; the Ministry of Health, Labor, and Welfare Sciences Research Grants; by a research grant on Health Science focusing on Drug Innovation from the Japan Health Science Foundation; by the program for promotion of Fundamental Studies in Health Science of the Pharmaceuticals and Medical Devices Agency; by a research grant for Cardiovascular Disease from the ministry of Health, Labor, and Welfare; and by a grant for Child Health and Development from the Ministry of Health, Labor, and Welfare.

#### REFERENCES

- Aurade, F., Pinset, C., Chafey, P., Gros, F., and Montarras, D. (1994). Myf5, MyoD, myogenin and MRF4 myogenic derivatives of the embryonic mesenchymal cell line C3H10T1/2 exhibit the same adult muscle phenotype. *Differentiation* 55, 185–192.
- Bischoff, R. (1994). The satellite cell and muscle regeneration. In: *Myology: Basic and Clinical*, ed. A. Engel, C. Franzini-Armstrong, and D. A. Fischman, New York: McGraw-Hill, Health Professions Division, 97–118.
- Cossu, G., and Mavilio, F. (2000). Myogenic stem cells for the therapy of primary myopathies: wishful thinking or therapeutic perspective? *J. Clin. Invest.* 105, 1669–1674.

- De Bari, C., Dell'Accio, F., Vandenabeele, F., Vermeesch, J. R., Raymackers, J. M., and Luyten, F. P. (2003). Skeletal muscle repair by adult human mesenchymal stem cells from synovial membrane. *J. Cell Biol.* 160, 909–918.
- Dezawa, M., Ishikawa, H., Itokazu, Y., Yoshihara, T., Hoshino, M., Takeda, S., Ide, C., and Nabeshima, Y. (2005). Bone marrow stromal cells generate muscle cells and repair muscle degeneration. *Science* 309, 314–317.
- Edmondson, D. G., and Olson, E. N. (1993). Helix-loop-helix proteins as regulators of muscle-specific transcription. *J. Biol. Chem.* 268, 755–758.
- Ervasti, J. M., and Campbell, K. P. (1991). Membrane organization of the dystrophin-glycoprotein complex. *Cell* 66, 1121–1131.
- Gerhart, J., Bast, B., Neely, C., Iem, S., Amegbe, P., Niewenhuis, R., Miklasz, S., Cheng, P. F., and George-Weinstein, M. (2001). MyoD-positive myoblasts are present in mature fetal organs lacking skeletal muscle. *J. Cell Biol.* 155, 381–392.
- Grounds, M. D., White, J. D., Rosenthal, N., and Bogoyevitch, M. A. (2002). The role of stem cells in skeletal and cardiac muscle repair. *J. Histochem. Cytochem.* 50, 589–610.
- Gussoni, E., Blau, H. M., and Kunkel, L. M. (1997). The fate of individual myoblasts after transplantation into muscles of DMD patients. *Nat. Med.* 3, 970–977.
- Hasty, P., Bradley, A., Morris, J. H., Edmondson, D. G., Venuti, J. M., Olson, E. N., and Klein, W. H. (1993). Muscle deficiency and neonatal death in mice with a targeted mutation in the myogenin gene. *Nature* 364, 501–506.
- Hawke, T. J., and Garry, D. J. (2001). Myogenic satellite cells: physiology to molecular biology. *J. Appl. Physiol.* 91, 534–551.
- Hoffman, E. P., Brown, R. H., Jr., and Kunkel, L. M. (1987). Dystrophin: the protein product of the Duchenne muscular dystrophy locus. *Cell* 51, 919–928.
- Imai, S., Fujino, T., Nishibayashi, S., Manabe, T., and Takano, T. (1994). Immortalization-susceptible elements and their binding factors mediate rejuvenation of regulation of the type I collagenase gene in simian virus 40 large T antigen-transformed immortal human fibroblasts. *Mol. Cell. Biol.* 14, 7182–7194.
- Kyo, S., Nakamura, M., Kiyono, T., Maida, Y., Kanaya, T., Tanaka, M., Yatabe, N., and Inoue, M. (2003). Successful immortalization of endometrial glandular cells with normal structural and functional characteristics. *Am. J. Pathol.* 163, 2259–2269.
- Mauro, A. (1961). Satellite cell of skeletal muscle fibers. *J. Biophys. Biochem. Cytol.* 9, 493–495.
- Mendell, J. R. *et al.* (1995). Myoblast transfer in the treatment of Duchenne's muscular dystrophy. *N. Engl. J. Med.* 333, 832–838.
- Miyoshi, H., Blomer, U., Takahashi, M., Gage, F. H., and Verma, I. M. (1998). Development of a self-inactivating lentivirus vector. *J. Virol.* 72, 8150–8157.
- Miyoshi, H., Takahashi, M., Gage, F. H., and Verma, I. M. (1997). Stable and efficient gene transfer into the retina using an HIV-based lentiviral vector. *Proc. Natl. Acad. Sci. USA* 94, 10319–10323.
- Mori, T. *et al.* (2005). Combination of hTERT and bmi-1, E6, or E7 induces prolongation of the life span of bone marrow stromal cells from an elderly donor without affecting their neurogenic potential. *Mol. Cell. Biol.* 25, 5183–5195.
- Nabeshima, Y., Hanaoka, K., Hayasaka, M., Esumi, E., Li, S., Nonaka, I., and Nabeshima, Y. (1993). Myogenin gene disruption results in perinatal lethality because of severe muscle defect. *Nature* 364, 532–535.
- Rodríguez, A. M. *et al.* (2005). Transplantation of a multipotent cell population from human adipose tissue induces dystrophin expression in the immunocompetent mdx mouse. *J. Exp. Med.* 201, 1397–1405.
- Rudnicki, M. A., Schnegelsberg, P. N., Stead, R. H., Braun, T., Arnold, H. H., and Jaenisch, R. (1993). MyoD or Myf-5 is required for the formation of skeletal muscle. *Cell* 75, 1351–1359.
- Sabourin, L. A., and Rudnicki, M. A. (2000). The molecular regulation of myogenesis. *Clin. Genet.* 57, 16–25.
- Schultz, E., and McCormick, K. M. (1994). Skeletal muscle satellite cells. *Rev. Physiol. Biochem. Pharmacol.* 123, 213–257.
- Seale, P., and Rudnicki, M. A. (2000). A new look at the origin, function, and "stem-cell" status of muscle satellite cells. *Dev. Biol.* 218, 115–124.
- Sicinski, P., Geng, Y., Ryder-Cook, A. S., Barnard, E. A., Darlison, M. G., and Barnard, P. J. (1989). The molecular basis of muscular dystrophy in the mdx mouse: a point mutation. *Science* 244, 1578–1580.
- Suda, J., Suda, T., and Ogawa, M. (1984). Analysis of differentiation of mouse hemopoietic stem cells in culture by sequential replating of paired progenitors. *Blood* 64, 393–399.
- Terada, N., Hamazaki, T., Oka, M., Hoki, M., Mastalerz, D. M., Nakano, Y., Meyer, E. M., Morel, L., Petersen, B. E., and Scott, E. W. (2002). Bone marrow cells adopt the phenotype of other cells by spontaneous cell fusion. *Nature* 416, 542–545.
- Terai, M., Uyama, T., Sugiki, T., Li, X. K., Umezawa, A., and Kiyono, T. (2005). Immortalization of human fetal cells: the life span of umbilical cord blood-derived cells can be prolonged without manipulating p16INK4a/RB braking pathway. *Mol. Biol. Cell* 16, 1491–1499.
- Wang, X., Willenbring, H., Akkari, Y., Torimaru, Y., Foster, M., Al-Dhalimy, M., Lagasse, E., Finegold, M., Olson, S., and Grompe, M. (2003). Cell fusion is the principal source of bone-marrow-derived hepatocytes. *Nature* 422, 897–901.

available at [www.sciencedirect.com](http://www.sciencedirect.com)[www.elsevier.com/locate/yexcr](http://www.elsevier.com/locate/yexcr)

## Research Article

# Single-cell-derived mesenchymal stem cells overexpressing Csx/Nkx2.5 and GATA4 undergo the stochastic cardiomyogenic fate and behave like transient amplifying cells

Yoji Yamada<sup>a</sup>, Kazuhiro Sakurada<sup>a,1</sup>, Yukiji Takeda<sup>b,2</sup>, Satoshi Gojo<sup>b,3</sup>, Akihiro Umezawa<sup>b,\*</sup>

<sup>a</sup>BioFrontier Laboratories, Kyowa Hakko Kogyo Co. Ltd., 3-6-6 Asahi-machi, Machida-shi, Tokyo 194-8533, Japan

<sup>b</sup>National Research Institute for Child Health and Development, 2-10-1 Okura, Setagaya-ku, Tokyo 157-8535, Japan

## ARTICLE INFORMATION

## Article Chronology:

Received 22 June 2006

Revised version received

31 October 2006

Accepted 15 November 2006

Available online 30 November 2006

## Keywords:

Mesenchymal stem cells

Cardiomyocytes

Transient amplifying cells

Csx/Nkx2.5

GATA4

## ABSTRACT

Bone marrow-derived stromal cells can give rise to cardiomyocytes as well as adipocytes, osteocytes, and chondrocytes *in vitro*. The existence of mesenchymal stem cells has been proposed, but it remains unclear if a single-cell-derived stem cell stochastically commits toward a cardiac lineage. By single-cell marking, we performed a follow-up study of individual cells during the differentiation of 9-15c mesenchymal stromal cells derived from bone marrow cells. Three types of cells, i.e., cardiac myoblasts, cardiac progenitors and multipotent stem cells were differentiated from a single cell, implying that cardiomyocytes are generated stochastically from a single-cell-derived stem cell. We also demonstrated that overexpression of Csx/Nkx2.5 and GATA4, precardiac mesodermal transcription factors, enhanced cardiomyogenic differentiation of 9-15c cells, and the frequency of cardiomyogenic differentiation was increased by co-culturing with fetal cardiomyocytes. Single-cell-derived mesenchymal stem cells overexpressing Csx/Nkx2.5 and GATA4 behaved like cardiac transient amplifying cells, and still retained their plasticity *in vivo*.

© 2006 Elsevier Inc. All rights reserved.

## Introduction

Cell-based therapy is a novel therapeutic strategy, based on the concept of the cell-mediated restoration of damaged or diseased tissue. Candidate cell sources include embryonic stem (ES) cells, hematopoietic stem cells (HSCs), neural stem cells (NSCs), mesenchymal stem cells (MSCs) [1], and so on. Clinical trials with MSCs have been performed in patients with

graft-versus-host disease through immunomodulatory effects [2], and osteogenesis imperfecta [3,4], and MSCs are expected to be one of the most available cells. The source of MSCs includes bone marrow [5], adipose tissue [6], umbilical cord [7] and placenta [8].

Bone marrow-derived stromal cells [9] can differentiate into mesenchymal progenitors, including osteoblasts [10], chondroblasts [11], skeletal myoblasts [12], adipoblasts [13],

\* Corresponding author.

E-mail address: [umezawa@1985.jukuin.keio.ac.jp](mailto:umezawa@1985.jukuin.keio.ac.jp) (A. Umezawa).

<sup>1</sup> Present address: Research Center, Nihon Schering K.K., 1-5-5 Minatojima-minamicho, Chuo-ku, Kobe-shi, Hyogo 650-0047, Japan.

<sup>2</sup> Present address: Department of General Medicine and Clinical Investigation, Nara Medical University, 840 Shijo-cho, Kashihara-city, Nara 634-8522, Japan.

<sup>3</sup> Present address: Department of Cardiovascular Surgery, Saitama Medical Center, 1981 Kamoda, Kawagoè, Saitama 350-8550, Japan.

and neurons [14,15] when placed in appropriate *in vitro* and *in vivo* environments. We have shown that bone marrow-derived stromal cells are also able to differentiate into cardiomyocytes *in vitro* and *in vivo* [13,14,16,17]. However, the characteristics of the cells that can differentiate into cardiomyocytes are poorly understood, and how the progeny of multipotent cells adopt one fate among several possible fates remains a fundamental question.

Hematopoietic stem cells are defined as cells that are capable of self-renewal to maintain a long-term supply of progeny and are capable of differentiating into multiple hematopoietic lineages [18]. Retroviral labeling of individual cells is one of the useful clonal assays to monitor lineage commitment at the single cell level [16,17,19]. At present, several models have been proposed in which hematopoietic lineage determination is driven intrinsically [20], extrinsically [21], or both [22]. We therefore performed retroviral labeling experiments of bone marrow-derived stromal cells to investigate whether cardiomyocytes are generated from committed cardiac precursor cells or uncommitted stem cells.

In the present study, we provide evidence that cardiomyocytes are stochastically differentiated from MSCs, and we demonstrate that forced expression of cardiomyocyte-specific transcription factors, *i.e.*, *Csx/Nkx2.5* and *GATA4*, destined these MSCs to a cardiomyocytic lineage.

## Materials and methods

### Cell culture

9-15c cells were used as a source of uncommitted stem cells in this study [23,24]. 9-15c cells are available through one of the cell banks (JHSF cell bank: [http://www.jhsf.or.jp/English/index\\_gc.html](http://www.jhsf.or.jp/English/index_gc.html); RIKEN cell bank: <http://www.brc.riken.go.jp/lab/cell/english/guide.shtml>). 9-15c cells were cultured using methods described previously [25]. The cells were cultured in Iscove's modified Dulbecco's medium (IMDM) supplemented with 20% fetal bovine serum and penicillin (100  $\mu\text{g}/\text{ml}$ )/streptomycin (100  $\mu\text{g}/\text{ml}$ )/amphotericin B (250  $\text{ng}/\text{ml}$ ) at 33°C with 5%  $\text{CO}_2$ .

Primary cultures of cardiac myocytes were prepared from the hearts of 16-day-old fetal C3H/HeJ mice (CLEA Japan, Inc., Tokyo, Japan) according to the method of Simpson *et al.* [26] with minor modifications. In brief, cardiomyocytes were dissociated into single isolated cells by trypsinization and the cells were plated in culture medium (IMDM with 20% fetal bovine serum).

### Cloning of *Csx/Nkx2.5* and *GATA4* cDNAs

The full open reading frames of mouse *Csx/Nkx2.5* and *GATA4* cDNAs were cloned by RT-PCR from poly(A) RNA obtained from the hearts of fetal mice using the following primers: *Csx/Nkx2.5*, sense: 5'-TGAAACCTGCGTGGCCAC-CATGT-3', antisense: 5'-GGCTCTTCCCTACCAGGCTCGG-3'; *GATA4*, sense: 5'-TAGTTCTGTCTGCCTCGTGCTCA-3', antisense: 5'-GGCGTGTATTACGGGTGATTATG-3'. The PCR products were subcloned into pGEM-T vector (Promega). DNA sequencing confirmed that the plasmids contained the full-

length fragments of the mouse *Csx/Nkx2.5* and *GATA4* coding regions.

### Retroviral transduction

The retroviral vectors pCLNCX (Imgenex), pCLPCX and pCLHCX were used. pCLPCX was constructed from pCLNCX by replacing the neomycin resistance gene with a puromycin resistance gene (pPUR; CLONTECH). pCLHCX was constructed from pCLNCX by replacing the neomycin resistance gene with a hygromycin resistance gene (pcDNA3.1/Hygro(+); Invitrogen). Fragments containing the EGFP, *Csx/Nkx2.5*, and *GATA4* genes were cloned into pCLNCX, pCLPCX, or pCLHCX. Each of these DNAs and pCMV-Eco (kindly provided by Nikunj Somia) were transfected into the producer cells (293 gag pol; kindly provided by Nikunj Somia) using TransFast (Promega). Two days after the transfection, the culture supernatant was filtered through a 0.45- $\mu\text{m}$  filter. 9-15c cells were treated with viruses and hexadimethine bromide (polybrene) (Sigma) (8  $\mu\text{g}/\text{ml}$ ) for 4–6 h. To generate stably expressing cells, 9-15c cells were cultured in the presence of 300  $\mu\text{g}/\text{ml}$  G418, 300  $\text{ng}/\text{ml}$  puromycin or 300  $\mu\text{g}/\text{ml}$  hygromycin. The mixtures of drug-resistant clones were used to average the clonal variation of the transfected gene expression.

### Cardiomyogenic induction

To induce differentiation, cells were initially plated at a density of  $2 \times 10^4$  cells/ml. The cells were treated with 3  $\mu\text{M}$  5-azacytidine (Sigma) for 24 h the next day. In some experiments, PDGF-BB (Peprotech) and retinoic acid (Sigma) were added to the culture dish coated with fibronectin (BD Biosciences) to give a final concentration of 10  $\text{ng}/\text{ml}$  and 1 nM, respectively, for 6 days. Total number of beating cells was estimated under phase contrast microscopy.

### RT-PCR

Total RNA was extracted from adult mouse hearts, skeletal muscles and cultured cells with an RNeasy kit (QIAGEN), and cDNA was made using the SuperScript First-strand Synthesis System (Invitrogen) from 1  $\mu\text{g}$  of total RNA. First-strand cDNA was diluted 20 fold and 1  $\mu\text{l}$  of cDNA was used for each PCR reaction. The following primer sets for cardiomyocyte-associated genes were used: atrial natriuretic peptide (ANP), sense: 5'-TTCTCGTCTGGCCTTTGG-3', antisense: 5'-GCTGGATCTTCGTAGGCTCCG-3'; cardiac troponin I (cTnI), sense: 5'-GATCCTGTCTCTGCCTCTGGA-3', antisense: 5'-TCATCCACTTTGTCCACCCGAG-3'; fast troponin I (fTnI), sense: 5'-GAAGCGCAACAGGCCATCAGC-3', antisense: 5'-CCACGTACCGCAGGTCCCGTTC-3'; *Csx/Nkx2.5*, sense: 5'-TGGCGTCTGGGGACCTGTCTG-3', antisense: 5'-GAGTCTGGTCTCTGCCGCTGTC-3'; *GATA4*, sense: 5'-TACATGGCCGACGTGGGAGCA-3', antisense: 5'-TGGAGT-TACCGCTGGAGGCAC-3'; exogenous *GATA4*, sense: 5'-CCAGAAAACGGAAGCCCAAGAA-3' (the sequence derived from mouse *GATA4* gene), antisense: 5'-GCTTGCCAAACCTA-CAGTGTTGG-3' (the sequence derived from pCLPCX vector); adiponectin, sense: 5'-CTGAAGAGCTAGCTCCTGCTTTG-3', antisense: 5'-GAAGAGAACGGCCTTGCTTC-3'; glyceraldehyde-



3-phosphate dehydrogenase (G3PDH), sense: 5'-CCCATCAC-CATCTTCCAGGAGC-3', antisense: 5'-TTCACCACCTTCTT-GATGTCATCATA-3'. G3PDH was used as an internal control. PCR was performed with TaKaRa Ex-Taq (TAKARA SHUZO CO., LTD) for 30–35 cycles, with each cycle consisting of 94°C for 1 min, 61–68°C for 1 min, and 72°C for 2 min, with an additional 7 min incubation at 72°C after completion of the final cycle.

RT-PCR samples were electrophoresed through agarose gels and stained with ethidium bromide and visualized through a UV light digital imaging system. Densities of electrophoresis bands were analyzed using ScnImage software (Scion Corporation).

#### Western blot analyses

Western blots were performed using whole-cell extracts according to the standard protocol [27]. Aliquots (30 µg) of whole-cell extracts were electrophoresed in SDS-polyacrylamide gels and transferred onto Immobilon-P polyvinylidene difluoride membrane (Millipore) by electroblotting. After treatment in blocking buffer, membranes were sequentially probed with the antibodies against Nkx2.5 (sc-8697, Santa Cruz) or Gata4 (sc-9053, Santa Cruz), and then with HRP-conjugated anti-goat or rabbit IgG. The bands were revealed using the ECL Plus standard protocol (Amersham Pharmacia Biotechnology).

#### Cellular transplantation

Following priming by 5-azacytidine for 24 h, the cells were cultured for an additional 3 days. Then the cells were harvested with 0.05% trypsin and 0.25 mM EDTA, and

suspended as single cells at a concentration of  $1 \times 10^5$  cells/µl with PBS. The cell viability in suspension, determined by 0.05% erythrosine dye exclusion, was 90% to 95%. After general anesthesia of the recipient mice by an intraperitoneal injection of 0.05 mg/g body weight pentobarbitone, cell transplantation was performed into the quadrant muscles of syngeneic adult recipient C3H/HeJ mice (CLEA Japan, Inc., Tokyo, Japan), aged 8 to 10 weeks old at a dose of  $1 \times 10^6$  and  $1 \times 10^8$  cells per mouse. All animals received humane care in compliance with the "Principles of Laboratory Animal Care" formulated by Keio University School of Medicine and the National Research Institute for Child Health and Development, and the experimental procedures were approved by the Laboratory Animal Care and Use Committee of Keio University School of Medicine.

#### Histological analyses

Tissues were fixed in 10% neutral buffered formalin and embedded in paraffin. Tissue sections (6 µm) were mounted on poly-L-lysine-coated slides. After deparaffinization with xylene, tissues were rinsed in acetone or ethanol. Slides were incubated in 0.3% H<sub>2</sub>O<sub>2</sub> for 30 min. After washing in PBS, tissues were preblocked for 30 min with 5% normal swine serum. They were incubated overnight at 4°C with mouse monoclonal antibody against recombinant GFP (CLONTECH Laboratories, Inc.) diluted 1:500. After rinsing in PBS, the slides were incubated with horseradish peroxidase-conjugated swine anti-mouse immunoglobulin diluted 1:100 with 1% BSA in PBS, and washed in cold PBS. Staining was developed using a solution containing DAB and 0.01% H<sub>2</sub>O<sub>2</sub> in 0.05 M Tris-HCl buffer, pH 6.7. Slides were counterstained with hematoxylin. Slices with positive signals for EGFP were further stained

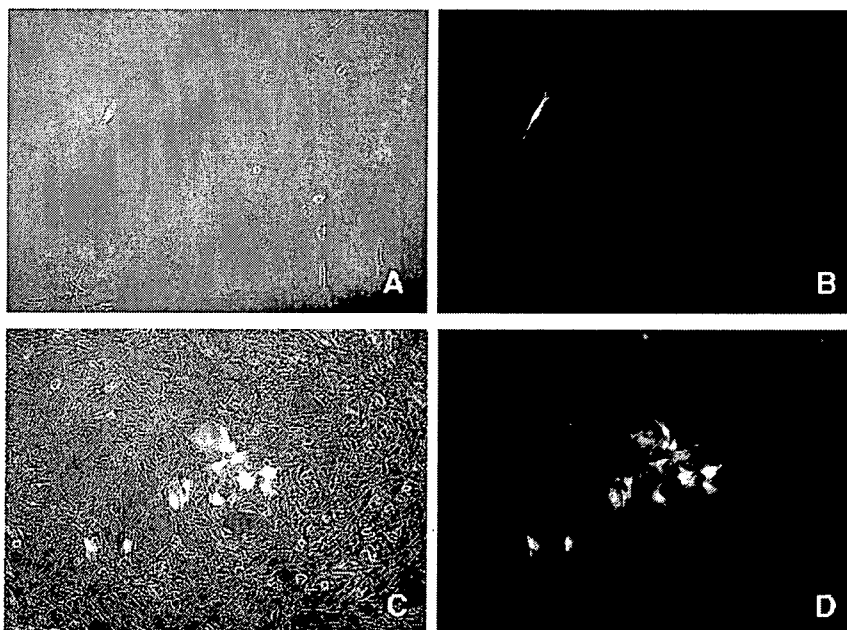


**Fig. 1** – Single cell marking by infection of retrovirus carrying EGFP. Phase contrast photomicrograph (A, C) and fluorescent photomicrograph (B, D) of 9-15c cells 1 day (A, B) or 7 days (C, D) after infection with retroviruses carrying EGFP. EGFP-positive single cell-derived cells were clustered.

with anti-CD31 (PECAM-1) antibody (M-20, Santa Cruz Biotechnology, Inc, California, USA).

Frozen sections (6  $\mu\text{m}$ ) of the samples were used to detect the donor cells and the differentiation status by examination under a fluorescence microscope. After fixation with acetone and blocking with PBS containing 5% rabbit serum, anti-CD31 or anti-desmin (Bio-Science Products AG, Switzerland) antibodies was used as the first antibody, and rat anti-mouse IgG antibody conjugated with tetramethylrhodamine isothiocyanate (T4280, Sigma, Missouri, USA) and goat anti-mouse IgG antibody conjugated with rhodamine (M116, Leinco Technology, Inc., MO, USA) were used as the second antibody, respectively.

## Results

### Single-cell marking of 9-15c cells

9-15c cells are mesenchymal stem cells [23,24] capable of differentiating into cardiomyocytes *in vitro* with the use of 5-azacytidine. To determine if cardiomyocytes were generated from committed cardiac precursor cells or uncommitted stem cells during the differentiation of 9-15c cells, we carried out a single-cell marking experiment. Following retrovirus-mediated EGFP gene infection, a single EGFP-labeled cell could be detected at Day 1 after infection (Figs. 1A, B). The fate of

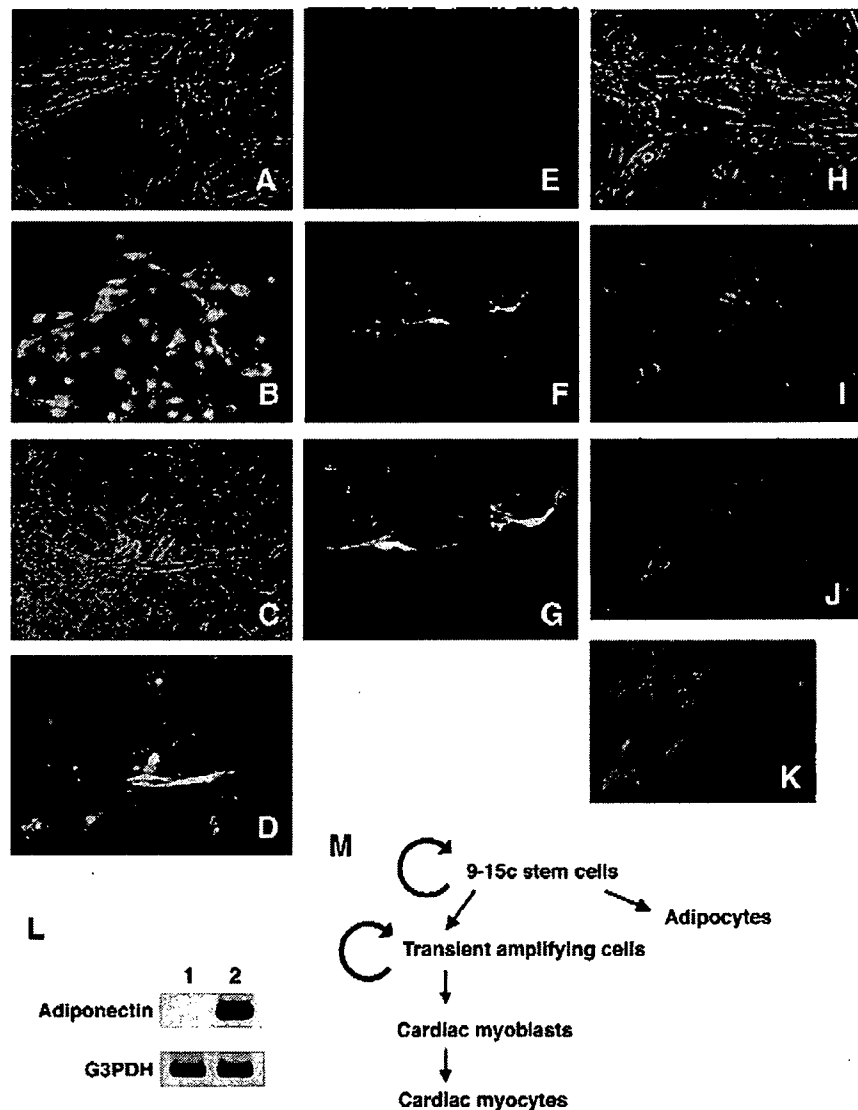


**Fig. 2** – Bipotency, i.e., cardiomyogenic and adipogenic differentiation, of single cell-derived cells. Single-cell-derived 9-15c cells marked by EGFP exhibited cardiomyogenic and adipogenic differentiation after exposure to 5-azacytidine. (A–B) Cardiomyogenic and undifferentiated EGFP-marked, single-cell-derived 9-15c cells; (C–G) Cardiomyogenic differentiation of EGFP-marked, single-cell-derived 9-15c cells; (H–J) Cardiomyogenic and adipogenic differentiation of EGFP-marked, single-cell-derived 9-15c cells. (A, C, E, H, J) Phase contrast photomicrographs; (B, D, F, G, I) fluorescent photomicrographs. (K) Enlargement of the panel J. (L) RT-PCR analysis of the adiponectin and G3PDH genes in 9-15c cells at the growing phase without any treatment (lane 1) and 4 weeks after exposure to 5-azacytidine (lane 2). (M) Scheme of 9-15c cell differentiation.

retrovirally tagged 9-15c cells could be traced by monitoring EGFP throughout the differentiation process after exposure to 5-azacytidine. Seven days later, the EGFP-positive, single-cell-derived cells were clustered (Figs. 1C, D). Four weeks after 5-azacytidine treatment, the EGFP-positive cells were examined for differentiated phenotypes. We identified beating cells as cardiomyocytes and oil-red-positive cells as adipocytes. Three kinds of cell populations were observed: a) a cell population in which cardiomyocytes and undifferentiated stem cells were EGFP-positive (Figs. 2A, B); b) a cell population in which all the EGFP-positive cells were cardiomyocytes (Figs. 2C–G); c) a cell population in which cardiomyocytes, adipocytes and undifferentiated stem cells were EGFP-positive (Figs. 2H–K). RT-PCR analysis shows that these cells express adiponectin (Fig. 2L), suggesting the presence of adipocytes among the differentiated population. These results imply that cardiomyocytes are generated from uncommitted stem cells (Fig. 2M).

#### 9-15c multipotent cells were preferentially destined to generate cardiomyocytes by forced expression of transcription factors *Csx/Nkx2.5* and *GATA4*

In order to elucidate the roles of *Csx/Nkx2.5* and *GATA4* in 9-15c cell differentiation, we infected 9-15c cells with retroviruses carrying *Csx/Nkx2.5* and *GATA4*. We detected *Csx/Nkx2.5* and *GATA4* gene expression in the infected cell by RT-PCR and Western blotting (Figs. 3A and B). *GATA4* gene was originally expressed in 9-15c; we detected the *GATA4* transgene with specific primers, but not the endogenous *GATA4* gene (Fig. 3A).

Four weeks after the induction of differentiation by 5-azacytidine treatment, we examined the efficiency of cardiomyogenic differentiation or the expression of cardiomyogenic markers. The expression of the ANP and cTnI genes was up-regulated in 9-15c cells overexpressing *Csx/Nkx2.5* and *GATA4* (9-15c-CG cells) compared to the uninfected 9-15c cells (Fig. 3C, lanes 5 and 9). When 9-15c-CG cells were treated with PDGF and retinoic acid on dishes coated with fibronectin in addition to 5-azacytidine, the expression of the ANP and cTnI gene was further up-regulated (Fig. 3C, lane 10).

#### Cell implantation into immunodeficient mice

To investigate whether 9-15c-CG cells differentiate *in vivo*, the cells treated with 10  $\mu$ M 5-azacytidine for 24 h were injected into immunodeficient mice (Figs. 4A–F). The donor cells clearly formed striated muscles without a branched structure as well as undifferentiated cells 81 days after implantation. The implanted 9-15c-CG cells clearly expressed desmin (Fig. 4G). The grafted cells also generated neovascularization near the injected site 1 month after injection; the EGFP-positive donor cells could be identified as the endothelium of these vessels (Fig. 4H). Immunohistochemistry with an antibody against CD31, a marker for endothelium, confirmed that the donor cells of the newly formed vessels had differentiated into endothelium (Fig. 4Hb). Engrafted donor cells appeared to maintain the characteristics of stem cells, that is, they continued to produce progeny, i.e., differentiated endothelial cells in this case.

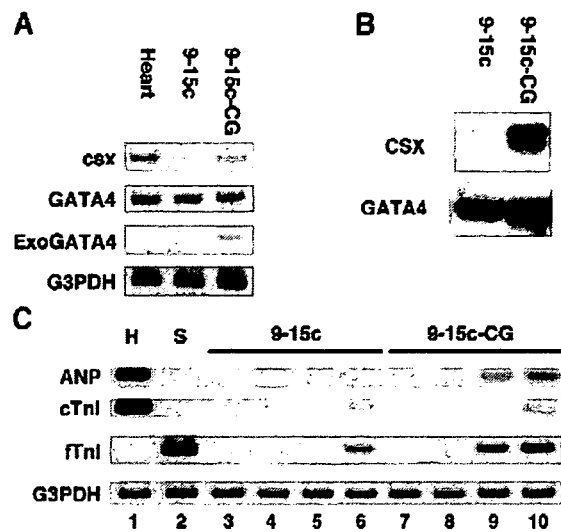


**Fig. 3** – Expression of cardiomyocyte-specific or associated genes in 9-15c cells. **A:** RT-PCR analysis of the *Csx*, *GATA4*, exogenous *GATA4* and *G3PDH* genes (from top to bottom) in adult mouse heart, 9-15c cells and 9-15c cells overexpressing the *Csx* and *GATA4* genes (9-15c-CG cells). **B:** Western blotting analysis of the *Csx* and *GATA4* proteins in 9-15c cells and 9-15c-CG cells. **C:** RT-PCR analysis of the *ANP*, *cTnI*, and *G3PDH* genes (from top to bottom) in 9-15c cells (lanes 3–6) and 9-15c-CG cells (lanes 7–10). 9-15c cells (lane 3) and 9-15c-CG cells (lane 7) were cultured without any treatment (lanes 4 and 8) or with exposure to 5-azacytidine alone (lanes 5 and 9), or 5-azacytidine, PDGF, retinoic acid, and fibronectin coating on a dish (lanes 6 and 10) for 4 weeks. Heart (lane 1: H) and skeletal muscle (lane 2: S) served as controls.

#### Enhancement of cardiomyogenic differentiation by the co-cultivation with cardiomyocytes

We co-cultured EGFP-labeled 9-15c-CG cells with cardiomyocytes of fetal mice *in vitro*. Four weeks after 5-azacytidine treatment, EGFP-positive beating cardiomyocytes were increased (Figs. 5A, B). To determine whether factors secreted from the cultured cardiomyocytes promoted cardiomyocytic differentiation, 9-15c cells and 9-15c-CG cells were cultured in growth medium supplemented with conditioned medium from cardiomyocyte cultures. The expression of the ANP and cTnI genes was up-regulated in both 9-15c cells and 9-15c-CG cells with exposure to the conditioned medium of cardiomyocyte cultures (Fig. 5C, lanes 3 and 7). Furthermore, treatment with PDGF and retinoic acid, and fibronectin coating on a dish enhanced cardiomyogenic marker expression in both 9-15c cells and 9-15c-CG cells (Fig. 5C, lanes 4 and 8).

#### Discussion

Different models arise from different conceptions of the MSCs as in hematopoietic stem cells' differentiation [28,29]. A hierarchical model of MSCs has been proposed based on the *in vitro* differentiation potential of human MSCs as observed

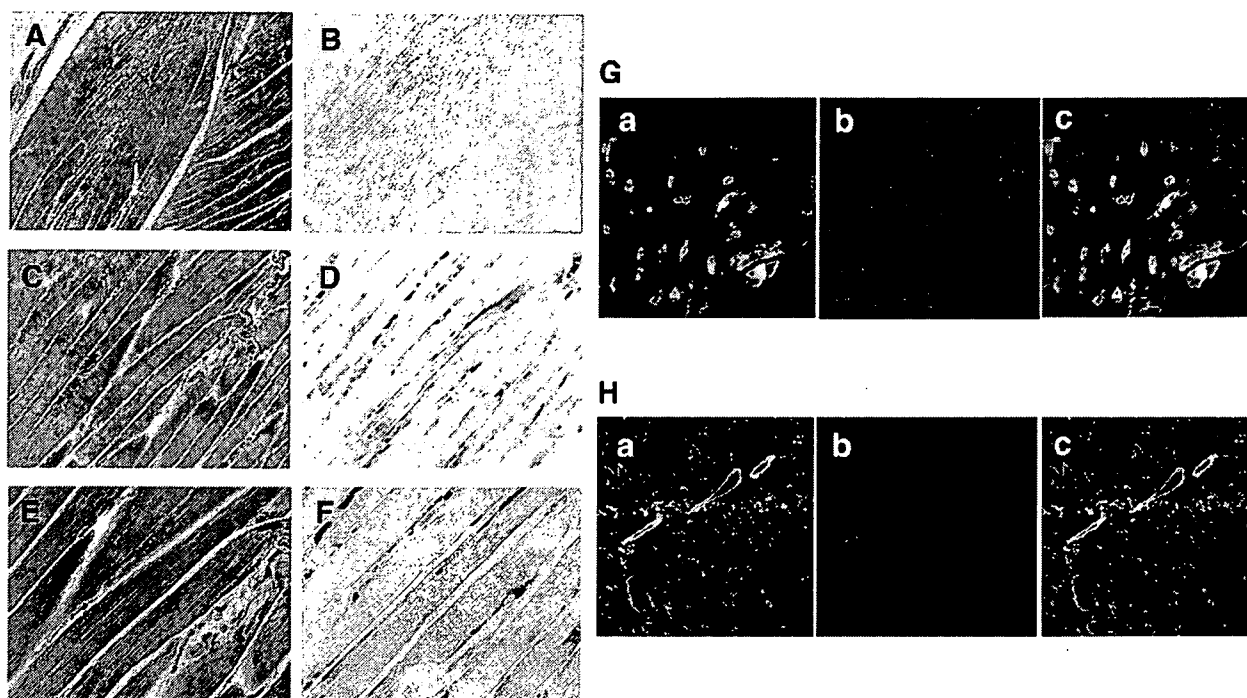


**Fig. 4** – Myogenic differentiation of the EGFP-labeled 9-15c-CG cells into the quadriceps femoris muscle. EGFP-labeled 9-15c-CG cells could be recognized morphologically as the skeletal myocytes in the quadriceps femoris muscle 3 months after transplantation (A, C, E: HE staining; B, D, F: immunohistochemistry using anti-GFP antibody). The EGFP-positive donor cells exhibited skeletal myocyte-specific features such as multiple nuclei in the periphery of the cells and striation. Generation of myocytes (G) and endothelial cells (H) by the EGFP-labeled 9-15c cells. The injected donor 9-15c cells labeled with EGFP were detected by green fluorescence. (Ga, Ha) Green fluorescence of EGFP-labeled donor cells. (Gb, Hb) Immunohistochemistry for desmin (Gb, red) or CD31 (Hb, red). (Gc, Hc) The merged images of green fluorescence of injected 9-15c cells and rhodamine of desmin or CD31 clearly demonstrated that 9-15c cells differentiated into myocytes or endothelium. A–F: Longitudinal section; G, H: Cross section.

by clonal analysis [30]. In the present study using single-cell marking, we found that 9-15c cells in culture consisted of a mixture of at least three types of cells, i.e., cardiac myoblasts, cardiac progenitors and multipotent stem cells. Cardiac myoblasts are defined as cells which can differentiate into only cardiac myocytes and have low proliferative potential; cardiac progenitors have proliferative capability and the ability to become cardiomyocytes; multipotent stem cells have both proliferative capability and multipotency. The results obtained in the present study suggest that 9-15c cells are stochastically committed toward the cardiac lineage, and that following this commitment they proliferate as transient amplifying cells and differentiate into cardiac myocytes through the differentiation process, and the hierarchical model applies in the case of 9-15c multipotent cells.

In the present study, we used 5-azacytidine to induce differentiation. 5-azacytidine is a cytosine analog that causes extensive demethylation. The demethylation is attributable to covalent binding of DNA methyltransferase to 5-azacytidine in the DNA [31], with the subsequent reduction of enzyme activity in cells resulting in random loss of methylation at many sites in the genome. Previously, it has been thought that 5-azacytidine activates cardiomyogenic master genes, such as Nkx2.5/Csx, GATA4, and MEF-2C, leading to stochastic trans-

differentiation of MSCs into cardiomyocytes [32,33]. This concept is difficult to account for the existence of cardiac progenitors and multipotent stem cells we identified, and we propose two possibilities how 5-azacytidine works. First, treatment of 5-azacytidine modulates heterochromatin remodeling and leads to dedifferentiation of 9-15c cells. Second, 9-15c cells are stochastically committed toward the cardiac lineage, being independent of treatment of 5-azacytidine. At this time we cannot conclude which is feasible, but it is certain cardiomyocytes are not only transdifferentiated by treatment of 5-azacytidine.

Csx/Nkx2.5 and GATA4 are two cardiac-enriched transcription factors that are expressed in precardiac mesoderm from the very early developmental stage [34,35]. In the present study, increased frequency of cardiomyogenic differentiation of 9-15c cells was successfully achieved *in vitro* by forced expression of Csx/Nkx2.5 and GATA4. These results are consistent with a report showing that both Csx/Nkx2.5 and GATA4 are required for the cardiac differentiation of P19CL6 cells derived from embryonic teratocarcinoma cells [36]. Cardiomyogenic differentiation, however, could proceed only after treatment with 5-azacytidine in our experimental setting, implying that Csx/Nkx2.5 and GATA4 are required but not sufficient for cardiac differentiation. Unknown factors

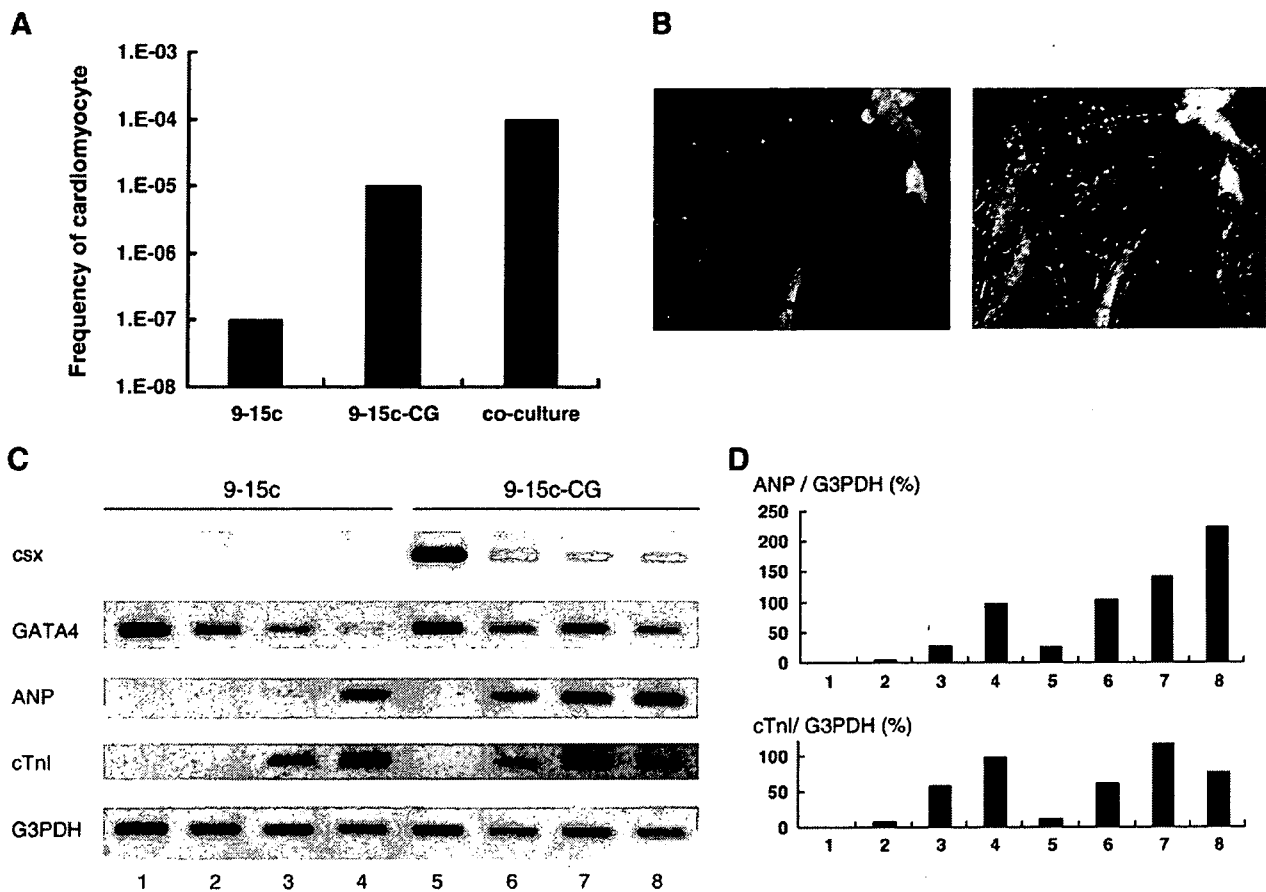


**Fig. 5** – Enhancement of cardiomyogenic differentiation of 9-15c cells by co-cultivation with murine fetal cardiomyocytes. **A:** Frequencies of cardiomyogenic differentiation in 9-15c cells, 9-15c cells overexpressing the *Csx* and *GATA4* genes (9-15c-CG cells), and 9-15c-CG cells co-cultured with murine fetal cardiomyocytes. **B:** Cardiomyogenic differentiation of EGFP-positive 9-15c-CG cells co-cultured with murine fetal cardiomyocytes. Left: Green fluorescence of EGFP-positive 9-15c-CG cells. Right: Same field visualized by phase-contrast microscopy merged with fluorescence image. **C:** RT-PCR analysis of the *Csx*, *GATA4*, *ANP*, *cTnI* and *G3PDH* genes in 9-15c cells (lanes 1–4) and 9-15c-CG cells (lanes 5–8). 9-15c cells (lane 1) and 9-15c-CG cells (lane 5) were cultured with exposure to 5-azacytidine alone (lanes 2 and 6) or 5-azacytidine and conditioned medium of cardiomyocyte cultures (lanes 3 and 7), or 5-azacytidine, conditioned medium of cardiomyocyte cultures, PDGF, retinoic acid, and fibronectin coating on a dish (lanes 4 and 8) for 4 weeks. **D:** Ratio mRNA expression level of *ANP* and *cTnI* to *G3PDH* in C. The mRNA level of 9-15c cells (lane 4) was regarded as equal to 100%.

induced by 5-azacytidine or microRNAs, whose key roles in stem cell biology are just emerging [37], also seem to be needed.

Adipogenic 3T3-L1 [38], osteogenic MC3T3-E1 [39], and chondrogenic ATDC5 cells [40] have been isolated from stem cells with a mesenchymal nature. In addition, cardiomyogenic precursors may be obtained from stem cells such as cardiac stem cells, embryonic stem cells, and mesenchymal stem cells. Fetal cardiomyocytes are differentiated cardiomyocytes, but not stem cells that can proliferate *in vitro*. Recently, cardiac stem cells capable of clonogenically self-renewing have been isolated from the adult heart [41–43]. Some cardiac stem cells also retain plasticity. The retention of plasticity, i.e., the ability to transdifferentiate into skeletal myocytes and endothelium, of 9-15c cells overexpressing *Csx/Nkx2.5* and *GATA4* supports the idea that these cells may be considered cardiac stem or amplifying cells in terms of differentiation and

self-renewal. On the other hand, *Csx/Nkx2.5* inhibits the myogenic differentiation of C2C12 cells and promotes neuronal differentiation [44]. This unexpected effect of *Csx/Nkx2.5* may be due to differential effects of the gene in different cell types, or of transient versus constitutive expression of the infected gene; dependency of the differentiated phenotypes on the gene expression period is observed for the *Notch* gene [45,46] and *noggin* gene [47].

Cell transplantation has been attempted to improve cardiac function in severe heart failure; MSCs have been transplanted to functionally restore damaged or diseased tissue in animal models, and mononuclear cells or myoblasts have been injected into ischemic hearts clinically. MSCs are capable of differentiating into many types of cells, and ‘cardiomyogenic master genes’ are able to enhance the commitment or determine the path to cardiomyogenic differentiation of these MSCs. The stemness of MSCs determined by single-cell